

# Integrating Fragment Assembly and Biophysical Methods in the Chemical Advancement of Small-Molecule Antagonists of IL-2: An Approach for Inhibiting Protein–Protein Interactions<sup>†</sup>

Brian C. Raimundo,\* Johan D. Oslob, Andrew C. Braisted, Jennifer Hyde, Robert S. McDowell, Mike Randal, Nathan D. Waal, Jennifer Wilkinson, Chul H. Yu, and Michelle R. Arkin\*

Sunesis Pharmaceuticals Inc., 341 Oyster Point Boulevard, South San Francisco, California 94080

Received January 9, 2004

Fragment assembly has shown promise for discovering small-molecule antagonists for difficult targets, including protein–protein interactions. Here, we describe a process for identifying a 60 nM inhibitor of the interleukin-2 (IL-2)/IL-2 receptor (IL-2R $\alpha$ ) interaction. By use of fragment-based approaches, a compound with millimolar affinity was evolved to a hit series with low micromolar activity, and these compounds were optimized into a lead series with nanomolar affinity. Fragment assembly was useful not only for hit identification, but also for lead optimization. Throughout the discovery process, biophysical methods and structural biology demonstrated that compounds bound reversibly to IL-2 at the IL-2 receptor binding site.

## Introduction

Interleukin-2 (IL-2) is a key mediator of the T-helper 1 (Th1) immune response.<sup>1–5</sup> Binding of IL-2 to the trimeric IL-2 receptor (IL-2R)—consisting of  $\alpha$  (IL-2R $\alpha$ ),  $\beta$  (IL-2R $\beta$ ), and  $\gamma$  chains (IL-2R $\gamma$ )—causes proliferation and clonal expansion of activated T cells. Abnormal Th1 immune responses have been implicated in graft rejection and other autoimmune diseases,<sup>6,7</sup> and current therapies target IL-2 production or the IL-2 signaling pathway.<sup>8,9</sup> Clinical data with antibodies directed against IL-2R $\alpha$  suggest that specific inhibition of the IL-2/IL-2R $\alpha$  interaction targets the Th1 response without causing the toxicity observed for more general immunomodulators.<sup>10,11</sup> Therapeutic antibodies have several drawbacks, however, including high cost-of-goods and lack of oral bioavailability. A small-molecule inhibitor of the IL-2/IL-2R $\alpha$  interaction could offer a significant improvement in immunosuppressive therapy. However, small molecule inhibitors of such protein–protein interactions have been difficult to identify.<sup>12–16</sup> This manuscript describes our research with IL-2, which we consider to be both an important therapeutic target for immune disease and a training ground for developing approaches toward small-molecule drug discovery at protein–protein interfaces.

Fragment-assembly approaches have been applied toward inhibitor discovery and optimization,<sup>17–23</sup> and we have been interested in using these methods for protein–protein interactions. First, small (<200 Da) organic molecules are screened for binding or inhibition against multiple subsites of a target. In a second step, selected fragments are chemically linked or otherwise optimized into a compound with sufficient activity to serve as a starting point for medicinal chemistry. Fragment assembly might be particularly useful for developing inhibitors of difficult targets such as protein–protein interactions. Fragment-based methods allow

screening of a very large virtual space while synthesizing a relatively small number of molecules and may therefore have an advantage over traditional screening approaches when hits are rare. Furthermore, since protein–protein interfaces tend to cover a large area of the protein surface, small molecule inhibitors might need to make a number of key binding interactions. Recently, it has been shown that, as the number of interactions needed for productive binding increases, the chances of finding a complimentary ligand–protein pair decreases dramatically; thus, complex binding sites are well-suited for a fragment-based approach.<sup>24</sup>

An important challenge with fragment assembly is the identification of the fragments, since they often have low (millimolar) affinity for the target. Methods to discover and validate fragments include NMR,<sup>18,19,25</sup> X-ray crystallography,<sup>22,26</sup> functional screening,<sup>27</sup> surface plasmon resonance (SPR),<sup>28,29</sup> and Tethering. (The term Tethering is a service mark of Sunesis Pharmaceuticals Inc. for its fragment-based drug discovery.)<sup>23,30</sup> In Tethering, fragments are selected based on disulfide-exchange between a cysteine-containing protein and disulfide-modified fragments (Figure 1). Each of these approaches has unique advantages, and we have used a number of methods in tandem to evolve inhibitors of IL-2.

IL-2 is one of the few protein hormones for which a small-molecule inhibitor has been described. Hoffman LaRoche has shown by NMR that the low micromolar inhibitor **1** (Figure 2) binds to IL-2 at the IL-2R $\alpha$  binding site.<sup>31,32</sup> Recently, we published the X-ray structure of **1** bound to IL-2 and characterized the binding site by Tethering.<sup>33</sup> The small-molecule binding site seen in Figure 2 contains two subsites. To the right is a shallow pocket containing the acidic residue Glu 62 that makes two hydrogen bonds with the guanidine moiety of **1**; to the left is a malleable, hydrophobic groove, created by the residues Arg 38, Leu 72, Lys 35, Met 39, and Lys 76, that binds to the biaryl portion of the compound. **1** can be seen as a merger of two

\* To whom correspondence should be addressed: raimundo@sunesis.com; mra@sunesis.com.

<sup>†</sup> We dedicate this manuscript to Miles Braisted and Joelle Morrow.

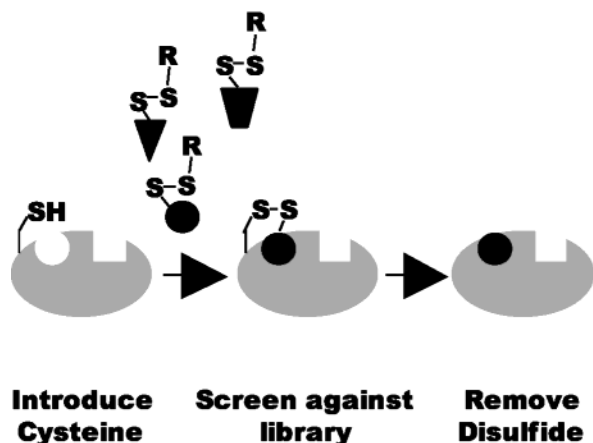


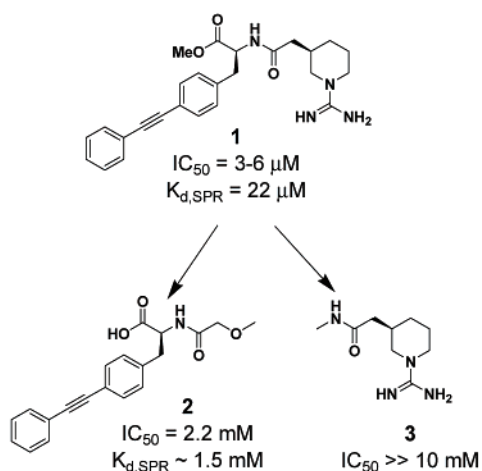
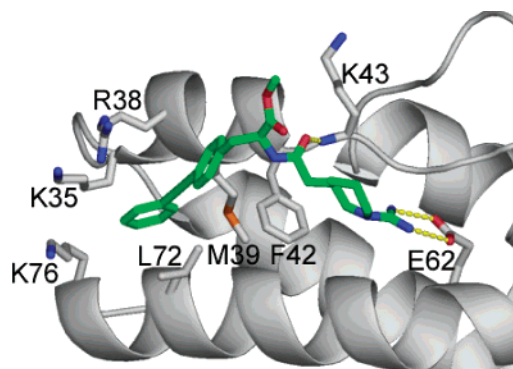
**Figure 1.** The Tethering method of fragment discovery is used to identify fragments that bind to a selected region of IL-2. In the first step, a cysteine mutation is placed near the binding site for IL-2R $\alpha$ . The protein is then interrogated with a pool of fragments that contain disulfide bonds, under conditions that favor disulfide exchange. After equilibrium has been reached, the compound/protein mixture is analyzed by mass spectrometry, which identifies the protein–small molecule conjugates. The highly reducing conditions ensure that only compounds with intrinsic affinity for the protein surface will be captured. In a separate step, the fragment can be prepared without a disulfide handle and tested for noncovalent binding to IL-2.

fragments—a biaryl acetylene amino acid (e.g., **2**) and a piperidinyl guanidine acetic acid (e.g., **3**)—joined by an amide bond. We chose to use this compound to develop tight-binding inhibitors of IL-2 using a fragment-based approach. The first step of our strategy was to determine whether fragments derived from **1** could be identified by various discovery approaches. The second step was to use these fragments to develop a new compound series that was chemically progressable and bound analogously to **1**. Finally, Tethering was used to identify an additional subsite adjacent to the known binding site of **1**. Incorporating fragments that target this subsite into our new series generated a molecule, **33i**, that inhibits IL-2/IL-2R $\alpha$  binding with an IC<sub>50</sub> of 60 nM and shows activity in a cell-based assay. Here we describe a highly integrated drug-discovery approach that combined fragment assembly, medicinal chemistry, biophysics, and structural biology to identify potent inhibitors of this important protein–protein interaction.

## Chemistry

**Biaryl Acetylene Dipeptides.** The first step in new lead generation was to replace the piperidinyl guanidine moiety on **1**. Starting with the biaryl acetylene **4**, a dipeptide guanidine fragment was introduced by standard peptide chemistry with Boc-amino acids (Scheme 1). Guanidine formation of **6** using *N,N*-bis-Boc-1-guanylpyrazole reagent, followed by Boc-deprotection and purification, led to **7a–m**.

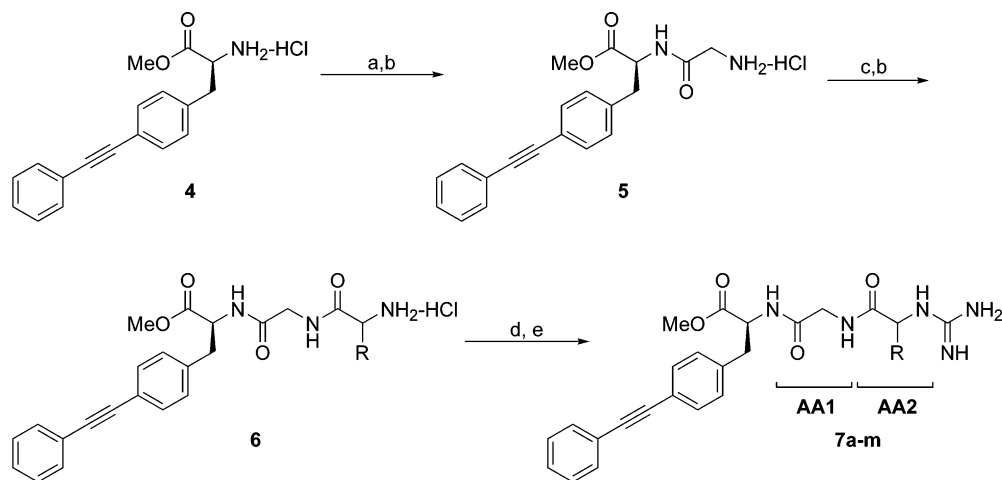
**Library Identifying New Hydrophobic Fragments.** To replace the biaryl moiety, the chemical sequence from Scheme 1 was inverted, starting with a preferred dipeptide fragment (AA2 = D-cyclohexylglycine) as an ‘anchor’ and incorporating ~100 lipophilic amines (Scheme 2). The activated ester **8** was used in a solution phase, parallel synthesis approach. A three-



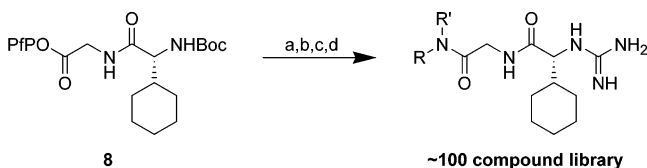
**Figure 2.** Fragments derived from **1**. Top, structure of **1** bound to IL-2 from X-ray crystallography (protein data bank ID code 1M48).<sup>33</sup> **1** shown in green sticks, with IL-2 shown in white ribbon. IL-2 residues comprising the binding site are shown in white sticks (oxygen atoms shown in red, nitrogen in blue, sulfur in orange). Bottom, structure of **1** and composite fragments (**2**, **3**). **2** was synthesized as the acid for solubility purposes; the acid derivative of **1** has the same activity as **1** itself (unpublished observations). Listed IC<sub>50</sub> data are average values from scintillation proximity assay (SPA); the listed K<sub>d,SPR</sub> value is from SPR measured at equilibrium for several concentrations of fragment (see Experimental Section).

step process of amine deprotection, guanidine formation, and guanidine deprotection was carried out in the same vial with removal of solvent in vacuo after each transformation. After final deprotection, each member of the library was purified by RP-HPLC.

**Phenyl Ring Substitution.** The most successful hydrophobic amine from Scheme 2 was a tricycle containing linked piperidine, pyrazole, and phenyl rings. Substitution of the phenyl ring was altered by synthesizing pyrazole triflate, **12**, and coupling it with substituted aryl boronic acids (Scheme 3). Starting with Boc-piperidine **9**, C-acylation with methyl cyanofornate provided **10**. Cyclization of **10** using hydrazine yielded pyrazolone **11**. Formation of the triflate and then Boc-protection of the pyrazole nitrogen provided **12**. Aryl boronic acids were coupled to the pyrazole using Suzuki reaction conditions and removal of the Boc-groups yielded piperidine **14**. Coupling aryl boronic acids with the triflate required Boc-protection of the pyrazole ring. Significant hydrolysis of the triflate was observed if the pyrazole ring was left unprotected. Transforma-

**Scheme 1.** Synthesis of Dipeptide Linkers for IL-2 Binding Molecules<sup>a</sup>

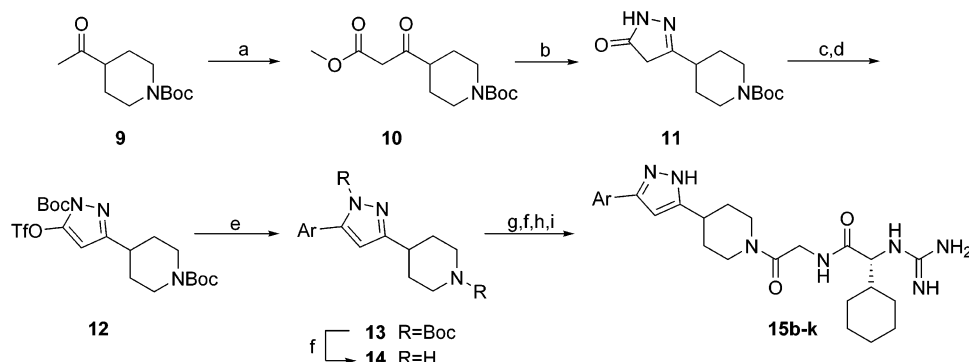
<sup>a</sup> (a) Boc-glycine, EDC, HOBT, Et<sub>3</sub>N in CH<sub>2</sub>Cl<sub>2</sub>; (b) HCl in dioxane; (c) Boc amino acid, EDC, HOBT, Et<sub>3</sub>N in CH<sub>2</sub>Cl<sub>2</sub>; (d) *N,N*-bis-Boc-1-guanylpyrazole, Et<sub>3</sub>N, MeOH; (e) TFA in CH<sub>2</sub>Cl<sub>2</sub>.

**Scheme 2.** Synthesis of Hydrophobic Fragment Library<sup>a</sup>

<sup>a</sup> (a) RR'NH, Et<sub>3</sub>N; (b) HCl in dioxane; (c) *N,N*-bis-Boc-1-guanylpyrazole, Et<sub>3</sub>N, MeOH; (d) TFA/CH<sub>2</sub>Cl<sub>2</sub> (1:1).

tion into the final compounds **15b–k** followed the same synthetic route as described for the general library (Scheme 2).

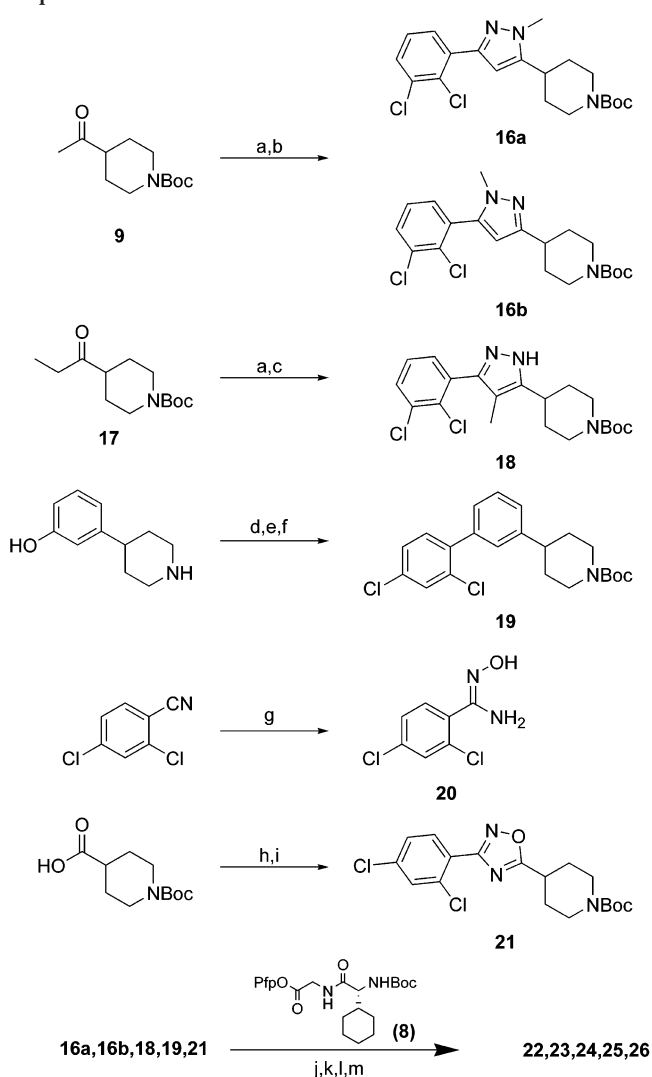
**Pyrazole Ring Substitution/Replacement.** As shown in Scheme 4, a methyl group was introduced at the three unsubstituted sites of the pyrazole by cyclization of diketone intermediates with the appropriate hydrazine. The synthesis of the *N*-methylated pyrazoles began by C-acylation of ketone **9**. Treatment of the diketone with methyl hydrazine provided the methyl pyrazoles **16a,b** as a mixture of regioisomers that were separated by chromatography. A series of NMR experiments were used to characterize each of the regioisomers. The C-methylated pyrazole, **18**, was synthesized by a similar sequence starting with ethyl ketone **17**.

**Scheme 3.** Synthesis of Substituted Phenyl Rings<sup>a</sup>

<sup>a</sup> (a) LHMDS, MeOCOCN, THF; (b) H<sub>2</sub>NNH<sub>2</sub>, EtOH, 70 °C; (c) PhN(Tf)<sub>2</sub>, Et<sub>3</sub>N, CH<sub>2</sub>Cl<sub>2</sub>; (d) Boc<sub>2</sub>O, Et<sub>3</sub>N, DMAP, CH<sub>2</sub>Cl<sub>2</sub>; (e) ArB(OR)<sub>2</sub>, PdCl<sub>2</sub>(PPh<sub>3</sub>)<sub>2</sub>, K<sub>2</sub>CO<sub>3</sub>, DMF/dioxane/H<sub>2</sub>O; (f) HCl in dioxanes; (g) **8**, Et<sub>3</sub>N, CH<sub>2</sub>Cl<sub>2</sub>; (h) *N,N*-bis-Boc-1-guanylpyrazole, Et<sub>3</sub>N, MeOH; (i) TFA/CH<sub>2</sub>Cl<sub>2</sub>.

Other tricyclic fragments contained replacements for the pyrazole ring (Scheme 4). The phenyl analogue **19** was synthesized from the commercially available piperidine phenol by protection, conversion to the triflate, and then Suzuki coupling. For oxadiazole **21**, hydroxybenzamidines **20** was condensed with the acid fluoride of Boc-isonipicotic acid to yield the desired tricycle. Completion of each analogue (**22–26**) followed the procedure described for the parallel library.

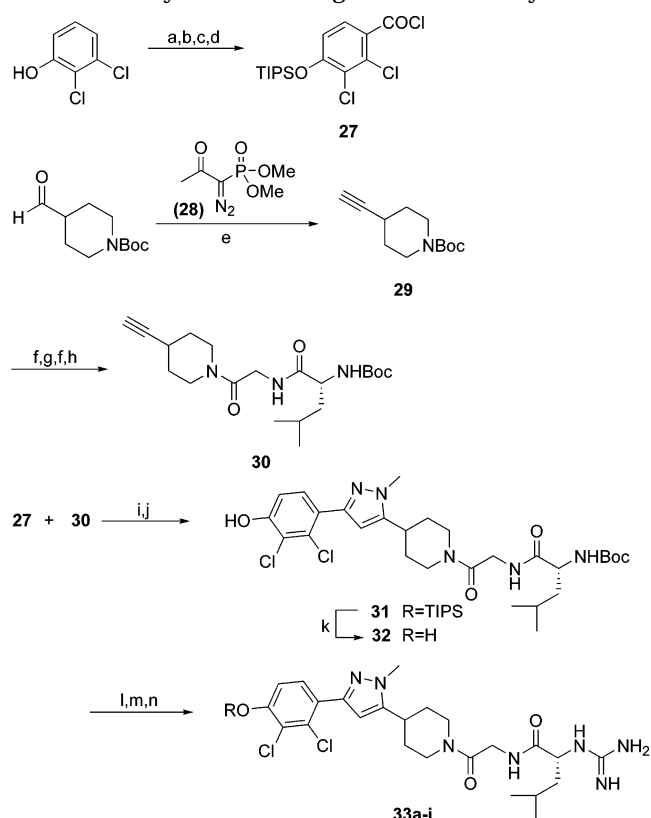
**Incorporation of Tethering-Derived Fragments and Synthesis of **33i**.** As shown in Scheme 5, fragments identified from Tethering (see below) were introduced through an ether linkage at the 4-position of the phenyl ring (relative to the pyrazole). At this stage, the original route for the synthesis of *N*-methylated pyrazoles was modified such that the 2-methylated pyrazole was obtained preferentially, as follows: Alkyne **29** was synthesized from an aldehyde derivative of isonipicotic acid by treatment with Bestmann's reagent. Palladium-mediated coupling of **29** and acid chloride **27** provided the alkynone which was treated with methyl hydrazine to yield the 2-methylated pyrazole as a single regioisomer. Deprotection of the phenol with TBAF yielded **32**. Incorporation of the fragments identified by Tethering was accomplished using standard alkylation or Mitsunobu conditions. Finally, the guanidine was installed as described above.

**Scheme 4.** Synthesis of Pyrazole Substitutions/Replacements<sup>a</sup>

<sup>a</sup> (a) LHMDS, methyl 2,3-dichlorobenzoate, THF; (b) MeNHNH<sub>2</sub>, MeOH; (c) H<sub>2</sub>NNH<sub>2</sub>, MeOH; (d) (Boc)<sub>2</sub>O; (e) Tf<sub>2</sub>NPh, Et<sub>3</sub>N, CH<sub>2</sub>Cl<sub>2</sub>; (f) 2,4-dichlorophenylboronic acid, Pd(PPh<sub>3</sub>)<sub>4</sub>, K<sub>2</sub>CO<sub>3</sub>, dioxane; (g) H<sub>2</sub>NOH, MeOH; (h) TFFH, Et<sub>3</sub>N, DMF; (i) **20**, THF; (j) HCl, dioxane; (k) **8**, Et<sub>3</sub>N, CH<sub>2</sub>Cl<sub>2</sub>; (l) *N,N*-bis-Boc-1-guanylpiperazine, Et<sub>3</sub>N, MeOH; (m) TFA in CH<sub>2</sub>Cl<sub>2</sub>.

**Results**

**Identifying Starting Fragment from 1.** The fragments **2** and **3** were derived from **1**, and the binding properties of each component were characterized (Figures 2, 3). Compound **2** inhibits the IL-2/IL-2R $\alpha$  interaction with an inhibition constant (IC<sub>50</sub>) of 2.2 mM. Binding of these compounds to IL-2 was monitored by SPR (see below for description of method). SPR data were in agreement with the inhibition assay and indicated a *K<sub>d</sub>* of approximately 1.5 mM for compound **2**. By contrast, no binding or inhibitory activity was observed for **3** at concentrations up to 10 mM. Using Tethering, we were able to detect covalent binding of a disulfide derivative of **3** to the Lys43Cys mutant of IL-2 (K43C-IL-2; Figure 3).<sup>33</sup> Fragment **2** was also derivatized with a disulfide-containing linker and tested for binding to K43C-IL-2. No conjugation was observed, however, suggesting that either the disulfide linker or the protein was not in a proper conformation for binding. Neither compound was detected by <sup>1</sup>H-<sup>15</sup>N

**Scheme 5.** Synthesis of Ring-Addition Library<sup>a</sup>

<sup>a</sup> (a) Br<sub>2</sub>, CH<sub>2</sub>Cl<sub>2</sub>; (b) TIPSCl, Et<sub>3</sub>N, THF; (c) *n*-BuLi, CO<sub>2</sub>, THF; (d) (COCl)<sub>2</sub>, DMF, CH<sub>2</sub>Cl<sub>2</sub>; (e) **28**, K<sub>2</sub>CO<sub>3</sub>, MeOH; (f) HCl in dioxane; (g) Boc-glycine, EDC, HOBT, Et<sub>3</sub>N, CH<sub>2</sub>Cl<sub>2</sub>; (h) Boc-D-leucine, EDC, HOBT, Et<sub>3</sub>N, CH<sub>2</sub>Cl<sub>2</sub>; (i) CuI, Et<sub>3</sub>N, Cl<sub>2</sub>(Ph<sub>3</sub>P)<sub>2</sub>Pd, toluene; (j) MeHNHNH<sub>2</sub>, EtOH; (k) TBAF, THF; (l) i. RX, Cs<sub>2</sub>CO<sub>3</sub>, DMSO, 65 °C or ROH, DEAD, PhP<sub>3</sub>, THF; ii. LiOH, THF, H<sub>2</sub>O, 60 °C; (m) *N,N*-bis-Boc-1-guanylpiperazine, Et<sub>3</sub>N, MeOH; (n) TFA in CH<sub>2</sub>Cl<sub>2</sub>.

HSQC NMR; in the case of **2**, precipitation was observed when compound and protein were combined at the millimolar concentrations required by the method. A combination of high-concentration screening and Tethering was therefore needed to identify the two fragments comprising **1**.

**Replacement of Piperidinyl Acetic Acid Linker.**

Having determined the binding properties of the two compounds comprising the inhibitor **1**, these fragments were used to identify a new series of inhibitors. The critical binding elements, the guanidine and biaryl-acetylene, were retained, and chemistry was focused on identifying linkers to replace the piperidine acetic acid. Ease of synthesis, the ability to generate analogues, and retention of the approximate length of the piperidine acetic acid were three major criteria used for prioritizing linker ideas. A dipeptide linker satisfied these criteria while offering the opportunity to alter the spatial relationship of the guanidine and biaryl acetylene.

A matrix of 18 compounds was synthesized as an initial set (Scheme 1) to probe conformation and linker length. Glycine, sarcosine, and  $\beta$ -alanine were incorporated at AA1 and six amino acids (glycine, alanine, D-alanine, sarcosine, proline, D-proline) were positioned at AA2. Representative data from the matrix are shown in Table 1. From this set, only one compound, **7c**, had an IC<sub>50</sub> < 300  $\mu$ M; equally important, the Hill slope for the inhibition curve was  $\sim$ 1, in sharp contrast to the

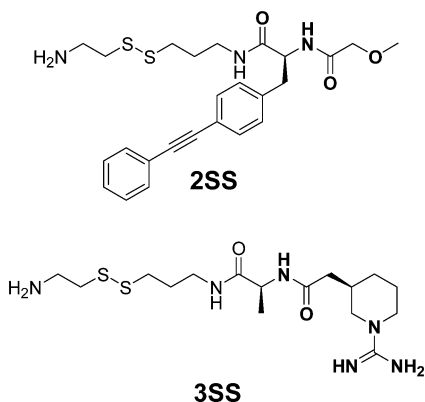
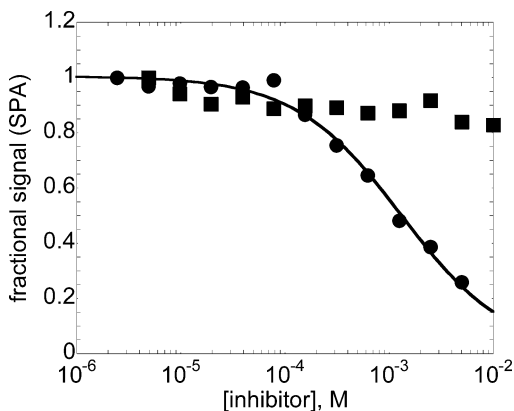


**Figure 3.** Top, Inhibition of IL-2/IL-2R $\alpha$  by fragments **2** (filled circles) and **3** (filled squares) shown by SPA (see Experimental Section). **2** has an IC<sub>50</sub> = 2.2 mM and a Hill slope  $\sim$  1. Bottom, disulfide derivatives of **2** and **3**. Tethering at K43C-IL-2 captured **3SS** but not **2SS**.

**Table 1.** Effect of Amino Acid Substitution on Inhibition of IL-2/IL-2R $\alpha$

compound	AA2	IC <sub>50</sub> ( $\mu$ M) <sup>a</sup>	slope <sup>b</sup>
<b>7a</b>	glycine	>2000	>2
<b>7b</b>	alanine	$\sim$ 2000	>2
<b>7c</b>	D-alanine	280	1.4
<b>7d</b>	sarcosine <sup>c</sup>	1200	3.5
<b>7e</b>	proline	1000	5.6
<b>7f</b>	D-proline	720	2.2
<b>7g</b>	D-valine	80	0.9
<b>7h</b>	valine	>2000	n.a. <sup>d</sup>
<b>7i</b>	D-Cha <sup>5</sup>	20	0.8
<b>7j</b>	D-Chg <sup>6</sup>	37	1.2
<b>7k</b>	D-Isoleucine	26	1.0
<b>7l</b>	<i>t</i> -Bu-alanine	9	1.4
<b>7m</b>	glutamine	900	1.8

<sup>a</sup> IC<sub>50</sub> values determined by ELISA,  $n \geq 2$ ; standard errors are within 2-fold of the reported value. <sup>b</sup> Hill slope in ELISA; a value of 1 is expected for single-site binding. <sup>c</sup> *N*-methyl glycine. <sup>d</sup> n.a. = not applicable. <sup>e</sup> Cyclohexylalanine. <sup>f</sup> Cyclohexylglycine.

other 17 compounds synthesized. Compounds **7a, b, d–f** had a Hill slope of  $\gg 1$ , suggesting an artifactual component—such as aggregation or precipitation—to the

**Table 2.** Effect of Terminal-Ring Substitution on Inhibition of IL-2/IL-2R $\alpha$

compound	R	IC <sub>50</sub> ( $\mu$ M) <sup>a</sup>
<b>15a</b>	2,4-Cl <sub>2</sub>	10
<b>15b</b>	H	120
<b>15c</b>	2-Cl	40
<b>15d</b>	3-Cl	130
<b>15e</b>	2,3-Cl <sub>2</sub>	10
<b>15f</b>	3,4-Cl <sub>2</sub>	110
<b>15g</b>	2-Me	50
<b>15h</b>	3-Me	150
<b>15i</b>	2,3-Me <sub>2</sub>	130
<b>15j</b>	2-Cl,4-OH	30
<b>15k</b>	2-Cl,4-OMe	50

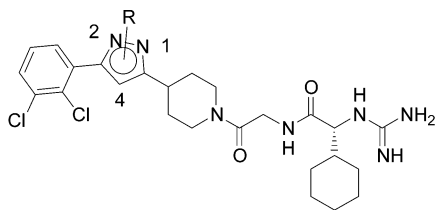
<sup>a</sup> Values determined by SPA.  $n > 2$ , Hill slopes =  $1 \pm \sim 0.2$  for all compounds.

inhibition. This information, with the support of additional biophysical characterization (see below), suggested that **7c**, although a weak inhibitor, functioned by blocking the IL-2R $\alpha$  site and was worthy of further optimization.

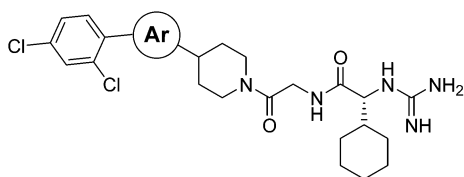
The synthetic flexibility of the dipeptide framework facilitated the rapid advancement of **7c** (Table 1). Neither polar side chains nor amino acids with the natural L-configuration were tolerated at the AA2 position. However, lipophilic, D-amino acids increased compound activity, with D-*tert*-butyl alanine (**7l**) giving a 30-fold increase in activity relative to D-alanine (**7c**). Replacement of glycine at the AA1 position or methylation of the two backbone nitrogen atoms did not improve activity. Overall, the SAR was well-defined, and within a set of  $\sim 15$  compounds a compound with an IC<sub>50</sub> < 10  $\mu$ M had been identified.

**Replacement of Hydrophobic Fragment.** In the third step toward discovering a lead series, alternate hydrophobic fragments were identified through synthesis of a solution-phase parallel library. Approximately 100 diverse primary and secondary amines, containing at least one aromatic ring and within a molecular weight range of 100–300, were coupled to the dipeptide guanidine fragment (Scheme 2). From this library, only a few compounds had an IC<sub>50</sub> < 200  $\mu$ M and all compounds in this active set incorporated bicyclic aromatic amines. Simple substituted benzyl or phenethylamines showed little or no inhibition of IL-2/IL-2R $\alpha$ , consistent with the hypothesis that activity requires occupation of both the guanidine-binding site and the lipophilic cleft. The most potent compound from the library, **15a** (Table 2), incorporated a tricyclic fragment containing a piperidine, aryl-pyrazole. The activity of **15a** (IC<sub>50</sub> = 10  $\mu$ M) and the synthetic versatility of the tricyclic framework made this compound a starting point for more detailed optimization.

**Optimization of the Hydrophobic Fragment.** To develop the SAR around library compound **15a**, we first investigated substitution around the phenyl ring (Table 2). Removing both chlorine atoms from the ring reduced activity more than 10-fold (**15b**), and this activity could

**Table 3.** Effect of Pyrazole Methylation on Inhibition of IL-2/IL-2R $\alpha$ 

Compound	R	IC <sub>50</sub> ( $\mu$ M)
15e	H	10
22	1-Me	20
23	2-Me	50
24	4-Me	400



Compound	Ar	IC <sub>50</sub> ( $\mu$ M) <sup>1</sup>
25		150
26		500

<sup>1</sup> Values determined by SPA. Hill slopes =  $1 \pm \sim 0.2$  for all compounds.

not be regained by replacement with other substituents. Introducing small substituents (methyl, chloro, fluoro) at the 2-position (**15c**, **15g**) improved activity  $\sim 3$ -fold, while single substitution at the 3- or 4-position were nonproductive (**15d**, **15h**). Activity was significantly decreased when larger substituents were introduced at any position (data not shown), and only the 4-position could tolerate heteroatom substitution (**15j**). Maintaining an IC<sub>50</sub> value below 10  $\mu$ M required incorporation of a chlorine atom at the 2-position as well as a second chlorine atom at either the 3- or 4-position. Interestingly, a modest change of substituents, such as replacement of the chlorine atoms with methyl groups (**15i**) resulted in significant loss of activity. The strong preference for dichloro substitution suggests that polarizable hydrophobic groups make favorable interactions with the protein surface and/or that these groups stabilize the bioactive conformation.

The central pyrazole ring was also a site of early chemical exploration (Table 3). A methyl group was introduced at the three unsubstituted positions of the ring in order to identify sites for further elaboration and to understand the conformational preference of the tricycle. The activity dropped only 2-fold when a methyl group was installed at the 1-position (**22**), but a more

**Table 4.** Biophysical Characterization of Binding of Compounds to IL-2<sup>a</sup>

compd <sup>b</sup>	IC <sub>50</sub> ( $\mu$ M) <sup>c</sup>	K <sub>d,SPR</sub> ( $\mu$ M) <sup>d</sup>	K <sub>d,AU</sub> ( $\mu$ M) <sup>e</sup>	<sup>15</sup> N, <sup>1</sup> H, HSQC <sup>f</sup>
<b>1</b>	7	19	20	+
<b>7c</b>	280	150	400	+
<b>7k</b>	26	70	50	n.t.
<b>7l</b>	9	15	4	+
<b>15a</b>	10	18	n.t.	+
<b>15e</b>	10	7	8 <sup>g</sup>	+

<sup>a</sup> Measurements are typically within 2-fold of the reported value. <sup>b</sup> See Figure 2 and Tables 1 and 2 for compound structures. <sup>c</sup> IC<sub>50</sub> values from ELISA,  $n \geq 7$ . <sup>d</sup> Determined by equilibrium binding as a function of compound concentration, see Experimental Section for details. <sup>e</sup> AU = analytical ultracentrifugation at sedimentation equilibrium; see Experimental Section for details. n.t., not tested. <sup>f</sup> Evidence for binding at the IL-2 hot spot by NMR, "+" indicates characteristic shifts observed for E62 and F42, among other residues. <sup>g</sup> Determined for close analogue, (AA2 = D-isoleu).

significant loss in activity was observed when the methyl group was introduced at the 2- or the 4-position (**23**, **24**); in particular, compound **24** showed a 400-fold loss in potency. Replacing the pyrazole with a phenyl or oxadiazole rings also resulted in a significant reduction in activity, suggesting that binding to IL-2 is highly sensitive to the shape of the tricycle.

**Binding of Compounds to IL-2.** Throughout the chemical optimization process, compounds were analyzed by SPR, analytical ultracentrifugation (AU), and NMR (Table 4; Figures 4–6). Experiments were designed to test whether the inhibition of IL-2/IL-2R $\alpha$  correlates with binding of compounds to IL-2 and to determine the reversibility and stoichiometry of binding at the IL-2R $\alpha$  binding site.

Binding of the compounds to IL-2 was characterized by SPR. By this method, a surface is labeled with IL-2 and the compounds are flowed over the chip's surface; binding of compounds causes a change in mass on the chip, which is detected by the change in reflectance units (RU). The kinetics of binding can be determined by monitoring the change in the SPR signal as a function of time. Each IL-2 inhibitor tested displayed rapid binding and dissociation kinetics, indicating that the compounds bind reversibly to IL-2 (Figure 4). The binding affinity and stoichiometry can also be determined by monitoring the RU as a function of compound concentration, since the RU value is directly proportional to the number of molecules binding to the surface of the chip (Figure 4). The compounds shown in Table 4 bind with 1:1 stoichiometry to IL-2; furthermore, the dissociation constants measured by SPR give the same rank-ordering of compounds as the inhibition assays, although the K<sub>d</sub> values tend to be slightly higher than the IC<sub>50</sub> values. Accuracy of the SPR data can be affected by nonspecific binding, which we did observe for this series of compounds at concentrations above  $\sim 500$   $\mu$ M (See Experimental Section).

Dissociation constants for small molecule/IL-2 interactions were also determined by equilibrium AU (Table 4 and Figure 5).<sup>34</sup> Varying ratios of compound and protein are spun in an analytical ultracentrifuge until sedimentation equilibrium is reached. The sedimentation curves are then measured by absorbance spectroscopy at wavelengths where the compound and/or protein absorb light. The shapes of the sedimentation curves determine the molecular weight of the protein, and the absorbance profile for the small molecule permits cal-

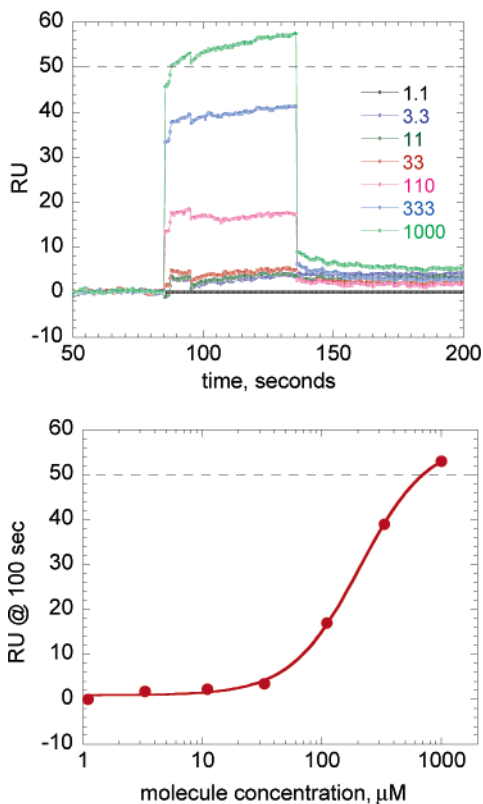


**Figure 4.** SPR measurement for the weak inhibitor **7c**. Top, sensorgram with background subtraction for **7c** binding to a CM5 chip labeled with 1700 RU of IL-2. The dotted line shows the RU of **7c** expected for 1:1 binding. The slope observed in the plateau region for 1000  $\mu\text{M}$  **7c** suggests nonspecific binding at this high concentration. Bottom, dose-response curve for the same SPR data. The binding RU at 100 s are plotted as a function of concentration of compound, and the resulting curve is fit by nonlinear regression. For this data set,  $K_{d,\text{SPR}}$  is calculated to be 150  $\mu\text{M}$ .

ulation of the  $K_d$  for the interaction. AU can also identify compounds that cause the protein to aggregate; the molecular weight of IL-2 was unchanged in the presence of inhibitors, indicating the absence of aggregation. From Figure 5, one can observe that the weakly bound compound **7c** ( $K_d = 400 \mu\text{M}$  by AU) shows less curvature than the more tightly bound compound **1** ( $K_d = 20 \mu\text{M}$  by AU). As shown in Table 4,  $K_d$  values obtained by AU provide the same rank-order of compounds as do the  $\text{IC}_{50}$  and SPR measurements.

$^1\text{H}$ - $^{15}\text{N}$  HSQC NMR spectroscopy was used to determine the binding site of **7c** and subsequent members in this chemical class. Figure 6 shows that the sub-millimolar compound **7c**, the low-micromolar inhibitor **7l**, and the tricyclic compound **15a** bind at the IL-2R $\alpha$  site in a manner similar to **1**.<sup>31,32</sup> As shown in Figure 2, Glu 62 and Phe 42 make direct contact with the small molecule; thus, the position of their NMR resonances serve as diagnostics for binding to the IL-2R $\alpha$  site. Moreover, the degree to which these resonances shift correlates with binding affinity of compound. Even the weakly bound compound **7c** induces a shift in Glu 62, indicating that molecules with an affinity in the 300  $\mu\text{M}$  range demonstrate specific binding at this site. Although all compounds bind at the same site, subtle differences in the NMR shifts of the dipeptide series (**15a**, **7l**) versus **1** indicate that the details of the binding contacts may

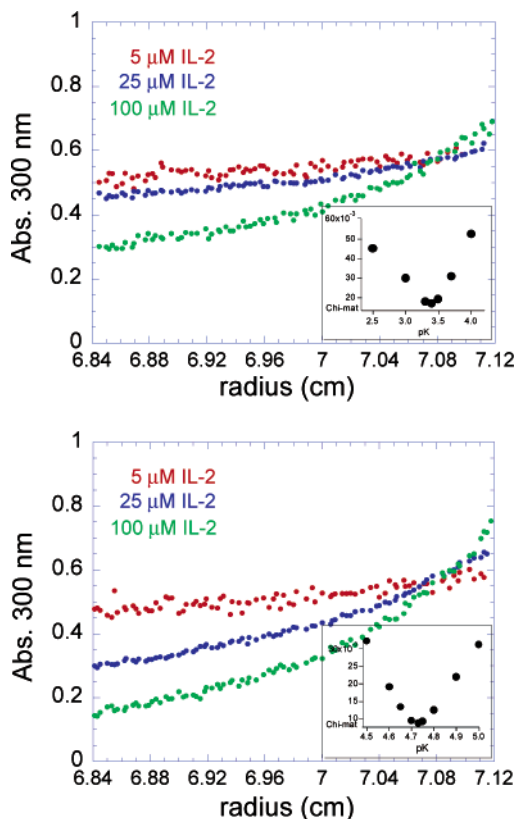


**Figure 5.** Determination of  $K_d$  by sedimentation equilibrium AU for **7c** and **1**. Top, sedimentation equilibrium curves for three ratios of **7c**:IL-2 at 25K RPM. Note that as concentration of protein is raised, the binding of compound increases, resulting in increased curvature. Inset, result of fitting AU data to determine  $K_d$ .<sup>34</sup> The minimum in the parabola gives the negative-log of the dissociation constant  $pK$ . For this data set,  $pK = 3.4$ ,  $K_d = 400 \mu\text{M}$ . Bottom, sedimentation equilibrium curves for three ratios of **1**:IL-2 at 25K RPM. Inset, result of fitting AU data to determine  $K_d$ . For this data set,  $pK = 4.7$ ,  $K_d = 20 \mu\text{M}$ . Compound concentration is 25  $\mu\text{M}$ ; protein concentrations are shown on the plots. Sedimentation curves are an average of five scans, measured in 0.003 mm increments. Extinction coefficients at  $\sim 300 \text{ nm}$ : IL-2,  $1000 \text{ M}^{-1} \text{ cm}^{-1}$ ; **7c**,  $22\,000 \text{ M}^{-1} \text{ cm}^{-1}$ ; **1**,  $13\,000 \text{ M}^{-1} \text{ cm}^{-1}$ . For experimental details, see Experimental Section.

vary, particularly in the region of the Glu 62-guanidine interaction.

**X-ray Structure of 15e.** The X-ray structure of **15e** bound to IL-2 confirms that this compound binds in a manner very similar to **1** (Figure 7),<sup>33,35</sup> though differences are observed in the guanidine-Glu 62 interaction. The guanidine of **15e** makes one hydrogen bond with Glu 62, while **1** makes two hydrogen bonds with this residue. The cyclohexyl group sits in a hydrophobic cleft formed by the side chains of Tyr 45, Lys 43, and Thr 111. This interaction explains the strong preference for lipophilic D-amino acids at AA2 and represents a new binding interaction not observed in the structure of **1** bound to IL-2. The dipeptide linker, in contrast to the piperidine acetic acid of **1**, makes minimal contact with the protein surface. However, in the hydrophobic site, the tricyclic fragment complements the lipophilic cleft, with each ring contacting the protein surface. Consistent with the SAR, methyl-group substitution is tolerated at the solvent-exposed 1-position of the pyrazole, but neither a methyl group nor a heteroatom can be accommodated at the buried 4-position (Table 3). Around the

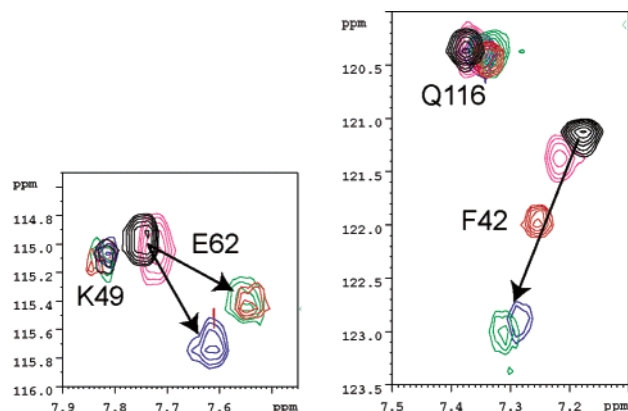


**Figure 6.**  $^1\text{H}$ - $^{15}\text{N}$  HSQC NMR spectra of IL-2 in the presence and absence of small-molecule inhibitors. Left,  $^1\text{H}$ - $^{15}\text{N}$  cross-peak corresponding to Glu 62 (E62). Right,  $^1\text{H}$ - $^{15}\text{N}$  cross-peak corresponding to Phe 42 (F42). NMR samples contain 200  $\mu\text{M}$  IL-2 uniformly labeled with  $^{15}\text{N}$  and 1% DMSO, in a buffer of 10 mM sodium acetate, pH 4.5. Spectra were measured at 40  $^\circ\text{C}$  in the presence of the following compounds: IL-2 only (black), 500  $\mu\text{M}$  **1** (blue), 2 mM **7c** (magenta), 500  $\mu\text{M}$  **7l** (green), and 500  $\mu\text{M}$  **15a** (red). In each case, the magnitude of the cross-peak shift correlates with binding affinity. Note that even the weak inhibitor **7c** causes Glu 62 and Phe 42 cross-peaks to shift, suggesting that this compound binds in the same site as **1**, **7l**, and **15a**. The placement of these residues in the small-molecule binding site of IL-2 is shown in Figures 2 and 7.

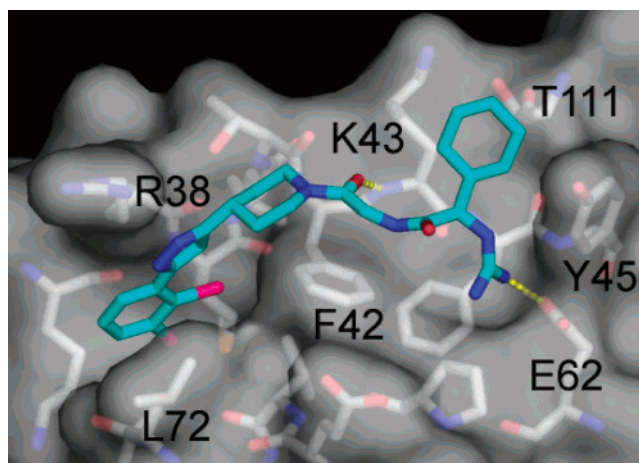


**Figure 7.** Structure of **15e** bound to IL-2 from X-ray crystallography (Protein Data Bank ID code 1PW6).<sup>35</sup> **15e** is shown in stick representation (carbon atoms in cyan, nitrogen in blue, oxygen in red, chlorine in pink); IL-2 is shown as a white surface. IL-2 residues within six angstroms of the compound are shown in stick representation (carbon atoms in white, nitrogen in blue, oxygen in red, sulfur in orange). Hydrogen bonds between the compound and protein are shown with yellow dashed lines (guanidine to Glu 62 and carbonyl oxygen to backbone nitrogen of Lys 43). Labeled IL-2 residues are discussed in the text and Figure 6. **15e** binds in the IL-2 $\alpha$  binding site determined by site directed mutagenesis.<sup>31,54,55</sup>

phenyl ring, both chlorine atoms bury into the protein surface, explaining the preference for small, lipophilic substituents at the 2- and 3-positions. The costructure of **15e** bound to IL-2 thus corroborates the SAR and biophysical data.

**Incorporation of Fragments from Tethering.** We applied Tethering to identify fragments that could complement the IL-2 $\alpha$  binding site and assist in compound optimization.<sup>29,33,36</sup> Ten individual cysteine

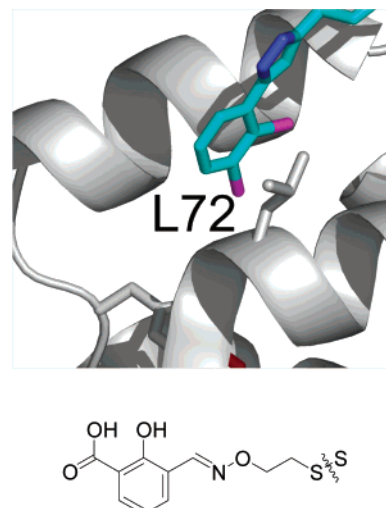


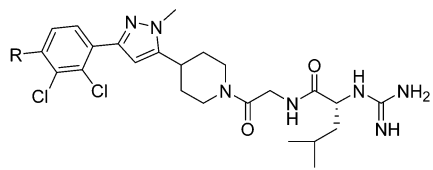
**Figure 8.** Position of Leu 72 and sample hit obtained at this residues by Tethering. Top, structure of **15e** (cyan) bound to IL-2 (white ribbon). Leu72Cys was used to identify fragments in the adaptive region adjacent to the binding site for **15e**. Bottom, strongly selected fragment from Leu72Cys. Statistical analysis shows a strong selection for small, aromatic, acidic fragments at this site.<sup>36</sup> Modeling of the salicylic acid fragment from Leu72Cys suggested that acidic fragments could be appended to **15e** at the 4-position through a two-atom linker.

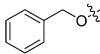
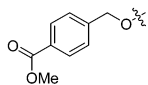
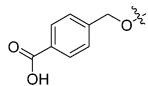
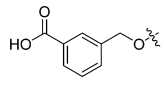
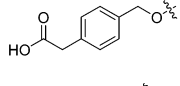
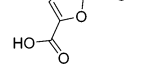
mutants of IL-2 were constructed and screened against a library of 7000 disulfide-containing fragments. Although these mutants were distributed around the two subsites, most of the hits were obtained from mutants targeting the lipophilic region. Aromatic acids were preferentially selected within this region; one example, a salicylate from Leu72Cys is shown in Figure 8.

Inspection of Leu 72 in the **15e**/IL-2 cocrystal structure suggested that these aryl carboxylic acids bind in the hydrophobic adaptive region adjacent to the binding site of **15e**.<sup>36</sup> Early SAR of the phenyl pyrazoles (Table 2) demonstrated that an ether was tolerated at the 4-position of the phenyl ring, thus providing a synthetically attractive handle and an appropriate vector for targeting this adaptive region. We first constructed a template compound that incorporated the preferred substitutions (2,3-dichloro substitution of the phenyl ring, 2-methylation of the pyrazole, and D-leucine at AA2) into one molecule. The resulting compound, **33c** (Table 5), had an  $\text{IC}_{50}$  value of 3.5  $\mu\text{M}$  and was used as the basis for further libraries.

In general, merging aryl acids onto compound **33c** resulted in a significant enhancement of activity (Table 5).<sup>36</sup> A carboxylate functionality was critical to achieving submicromolar activity, although its exact placement about the aromatic ring was found to be less important. Addition of a benzoic acid fragment resulted in an  $\text{IC}_{50}$  of 200 nM (**33f**). Removing the carboxylate (**33d**) or masking it as the methyl ester (**33e**) reduced activity by more than 100-fold. Shifting the carboxylate to the meta-position (**33g**) or extending the carboxylate by one methylene unit (**33h**) resulted in a modest loss of activity. Of the 20 compounds synthesized, eight had an  $\text{IC}_{50} < 1 \mu\text{M}$ . The most potent compound, **33i**, incorporated a furanoic acid moiety and had an  $\text{IC}_{50} = 60 \text{ nM}$ . Thus, Tethering provided information about the preferred binding elements at the adaptive region that, in turn, directed the chemical optimization. Synthesiz-



**Table 5.** Effect of Addition of Aryl Carboxylic Acids on Inhibition of IL-2/IL-2R $\alpha$ 


Compound	R	IC <sub>50</sub> ( $\mu$ M) <sup>1</sup>
33a	H	2.0
33b	OH	8.1
33c	MeO	3.5
33d		35
33e		40
33f		0.2
33g		0.4
33h		0.6
33i		0.06

<sup>a</sup> Values determined by SPA. Hill slopes =  $1 \pm \sim 0.2$  for all compounds.

ing a small set of compounds defined by the Tethering data led to a 30-fold increase in activity.

**X-ray Structure of 33i.** The X-ray crystal structure of **33i** bound to IL-2, shown in Figure 9, supports the design strategy and explains the observed SAR.<sup>35</sup> As expected, **33i** binds analogously to **15e** (Figure 7). One striking difference in the structure of **33i** is the guanidine moiety, which adopts a conformation very similar to that of **1** (Figure 2) and makes two hydrogen bonds to Glu 62. The greater flexibility of the D-leucine side chain relative to the D-cyclohexyl glycine of **15e** probably allows for this reorientation of the guanidine. There are also minor differences in the orientation of the tricycle within the hydrophobic cleft. The furanoic acid moiety is bound in a shallow pocket next to the hydrophobic cleft and is surrounded by the positively charged side chains of Arg 38 and Lys 35. These side chains are not well-ordered in the X-ray structure, and there are no apparent hydrogen bonds between the carboxylate and the protein. Rather, it appears that the increased affinity seen for **33i** is due to the complimentary electrostatic potentials of the negatively charged acid and the positively charged surface of IL-2 in this region (unpublished observations). This notion is supported by the observed SAR, since the specific placement of the

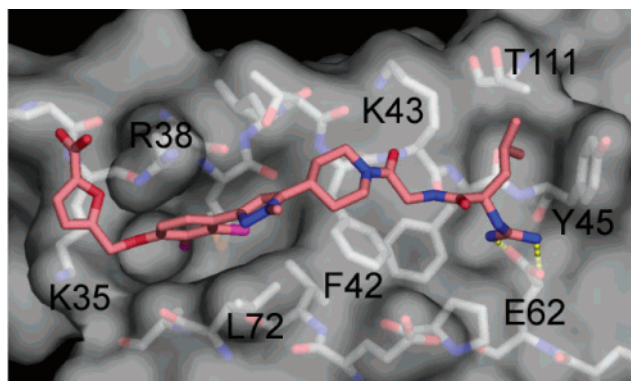


**Figure 9.** Structure of **33i** bound to IL-2 from X-ray crystallography (Protein Data Bank ID code 1PY2).<sup>35</sup> **33i** is shown in stick representation (carbon atoms in pink, nitrogen in blue, oxygen in red, chlorine in dark pink); IL-2 is shown in surface representation, and residues within 6 Å of **33i** are shown in stick form (carbon atoms in white, nitrogen in blue, oxygen in red, sulfur in orange). Hydrogen bonds between the compound and protein are shown with yellow dashed lines (guanidine to Glu 62, carbonyl oxygen to the backbone nitrogen atom of Lys 43). **33i** binds similarly to **15e** (Figure 7), at the binding site for IL-2R $\alpha$  determined by site-directed mutagenesis.<sup>31,54,55</sup> Note that the furanoic acid binds in a groove formed by the positively charged residues Arg 38 and Lys 35. Labeled residues are discussed in the text.

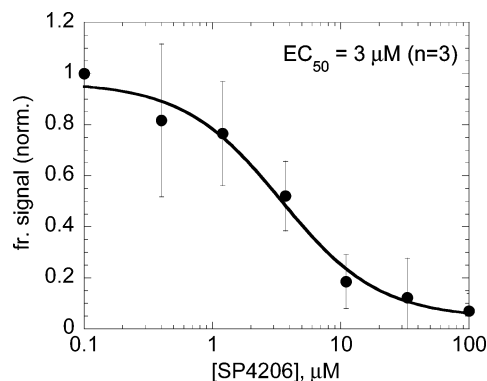


**Figure 10.** Inhibition of IL-2 dependent, STAT-5 phosphorylation in the presence of **33i**. STAT-5 phosphorylation was monitored by Western blot, using an anti-phosphotyrosine antibody, an alkaline-phosphatase-labeled secondary antibody, and a luminescent substrate. Luminescence was recorded on film and quantified by densitometry, and reduction in band intensity was plotted as a function of compound concentration. Data shown are an average of three separate experiments.

acidic group has only a minor effect on the activity of compounds in this series.

**Biological Properties of 33i.** **33i** was tested for IL-2 antagonism in a cell-based assay. Human IL-2 binds to mouse IL-2R expressed on the surface of the murine T cell line CTLL-2. IL-2 activates intracellular signaling, which leads to phosphorylation of the transcription factor STAT5.<sup>37</sup> In the presence of **33i**, phosphorylation of STAT5 is reduced in a dose-dependent manner with an EC<sub>50</sub> = 3  $\mu$ M (Figure 10). In the same assay, **1** shows little inhibition of STAT5 phosphorylation at 100  $\mu$ M concentration, **33a** gives an EC<sub>50</sub>  $\sim$  25  $\mu$ M, and soluble IL-2R $\alpha$  has an EC<sub>50</sub>  $\sim$  30 nM (3–10-fold weaker than observed in SPA and ELISA). As a control, the inhibition of IL-15 signaling was measured. IL-15 signals through a trimeric receptor that includes the  $\beta$  and  $\gamma$  chains of IL-2R, but the IL-15-specific chain IL-15R $\alpha$ ;<sup>3</sup> therefore, compounds that bind to IL-2 at the IL-2R $\alpha$  site should

have no effect on IL-15 signaling. As expected, **33i** and IL-2R $\alpha$  were inactive against IL-15-mediated phosphorylation of STAT5.

The in vitro and in vivo pharmacokinetic properties of **33i** were also analyzed. In the presence of human liver microsomes, the compound was found to be stable, with 80% ( $\pm 1\%$ ,  $n = 2$ ) remaining after 60-min incubation at 37 °C. The pharmacokinetic properties in mice were also favorable, with the compound showing a 2.1 h terminal half-life, a clearance rate of 13.6 mL/min/kg, and a volume of distribution at steady state ( $V_{ss}$ ) of 1.1 L/kg.

## Discussion

**Fragment Characterization.** To fulfill the potential of fragment assembly, robust methods must be developed for identifying the fragments, characterizing their binding, and linking them productively. As a proof-of-concept for fragment identification, we began with a known small-molecule ligand and examined its component fragments for binding to IL-2. These two fragments represent two different classes of molecules. Compound **2** is hydrophobic and binds in an adaptive region of the protein, while compound **3** is hydrophilic and binds in a shallow, preformed pocket utilizing a hydrogen bond network. Given these structural differences, it is not surprising that different fragment screening methods are needed to identify these compounds.

Fragment **2** has millimolar activity in functional screens (SPA, ELISA) and in a binding assay (SPR) but was not captured by Tethering at K43C-IL-2. This result is consistent with the structural data on IL-2; without ligands or with disulfide-bound fragments,<sup>29,33,38,39</sup> Phe 42 is found in an "up" conformation, acting as a wall between the hydrophilic and hydrophobic subsites. Thus, a fragment bound at Lys43Cys would be prevented from binding the hydrophobic site. Tethering does capture numerous fragments when the cysteine mutant is placed on the other side of Phe 42, and these hits recapitulate the hydrophobic, aromatic properties of the biaryl acetylene.<sup>29,33</sup>

In contrast to **2**, fragment **3** did not show activity in functional assays, suggesting that its binding affinity is weaker than that of **2**. However, **3** was captured by Tethering at K43C-IL-2. Binding of fragments in the hydrophilic site requires satisfying a number of hydrogen bonds within certain geometric constraints. Furthermore, highly soluble fragments have little energy to release by binding to the protein, and thus inherent affinities may be low. Tethering facilitates binding of such fragments by augmenting the affinity through formation of a reversible covalent bond. In general, we find that a combination of fragment discovery methods is more successful in finding a range of fragment structures than any one method alone.

**Evolving Fragments to Hits.** Often, the most difficult step in fragment assembly is advancing compounds from millimolar to micromolar affinity. For IL-2, the starting point was a hydrophobic fragment with millimolar affinity, and the parameters that defined the adjacent hydrophilic binding site were known. Within these boundaries and using a modular chemical approach, we readily attained a 10-fold improvement in activity and recaptured the Glu 62-guanidine binding

interaction. From there, efficient optimization of the dipeptide linker further boosted affinity by incorporating a new binding element (hydrophobic D-amino acid). Throughout the process, these low-affinity compounds demonstrated the correct behavior profile, including inhibition curves with Hill slopes close to 1, solubilities in excess of the IC<sub>50</sub> value, and evidence for reversible, low stoichiometry binding. The process of evolving fragments to micromolar hits was successful because the recognition requirements and shape of the binding site were known, the chemical strategy allowed rapid parallel synthesis, and early characterization ensured that weak inhibitors bound in the desired site on IL-2.

**Compound Advancement through Tethering.** Fragment discovery tools are typically used to identify new starting points for chemistry,<sup>18–20,22,23</sup> but they can also be helpful for optimizing a chemical lead series.<sup>21,40</sup> Here, Tethering identified a class of fragments that bound in a new site adjacent to the known ligand-binding site. Incorporation of these fragments into the existing lead series led to a dramatic increase in binding affinity.

Tethering greatly facilitates lead optimization by providing information on the location of the fragments' binding site.<sup>23</sup> Although it was difficult to model the binding modes of fragments selected in the flexible hydrophobic region, it was straightforward to estimate the *distance* between the disulfide-bound fragments and the terminal phenyl ring of the tricyclic compound given the relatively fixed position of Leu 72.<sup>33,36</sup> The design strategy was supported by the activity data, since all of the aromatic acids attached by an ether linker to **33c** led to improved potency. It is noteworthy that early SAR around the tricycle did not uncover additional binding affinity. This may not be surprising, given that an activity boost required a large step in compound complexity, with a carboxylic acid and aromatic ring properly connected to the scaffold. Fragment-based approaches can be especially valuable for identifying complex binding elements adjacent to known binding sites. Tethering provides a useful way to interrogate these novel subsites without requiring detailed knowledge of the protein conformation.

**IL-2 as Test Case for Protein–Protein Interactions.** Historically, protein–protein interactions have been difficult to inhibit with small, organic molecules, although some successes have been reported.<sup>12–16</sup> One likely reason for this general intractability is the structure of protein surfaces; in crystal structures of protein–protein pairs, the interfaces tend to be rather flat and lacking the deep pockets and grooves seen in more traditional drug targets such as enzymes and G-coupled protein receptors.<sup>41–43</sup> On the other hand, work with IL-2 and other proteins indicates that these protein surfaces can be highly adaptive<sup>29,33,44–48</sup> and might therefore contain transient structures that are amenable to small-molecule binding.

The importance of IL-2 adaptivity in small-molecule recognition is highlighted by the structures of **15e** and **33i** bound to IL-2. The surface of IL-2 undergoes numerous structural adaptations that are only observed when small molecules are bound. For example, Phe 42 is always found in an up-position in the absence of **1**, **15e**, and **33i**.<sup>29,33,35,38,39</sup> In the presence of these ligands,

Phe 42 rests against the protein surface, where it provides a binding surface for the small molecule. There are also small rearrangements around the hydrophilic site upon binding of the lipophilic D-amino acid in **15e**. The hydrophobic region also adapts upon small-molecule binding, maintaining a similar conformation when bound with ligands **1** and **15e**. In the costructure of **33i**, there appears to be a further organization of the site occupied by the furanoic acid,<sup>35</sup> and this conformation could maximize the electrostatic interactions between the acid and basic side chains on IL-2. Thus, at each stage in the small-molecule discovery process, the structure of IL-2 is seen to change in response to new binding elements introduced onto the molecule. Identifying and targeting adaptive regions of structure might therefore be a valuable approach for inhibitor discovery at protein interfaces.

Another reason that few drug leads have emerged for protein-protein targets could be the prevalence of screening hits that inhibit by an unacceptable mechanism. While screening artifacts can arise for any target, they might be more difficult to characterize for protein-protein systems, where powerful tools such as enzyme kinetics are not available. In characterizing inhibitors of IL-2, therefore, we considered it important to demonstrate that inhibition resulted from single-site binding at the IL-2R $\alpha$  binding site. It is noteworthy that hydrogen bond interactions between Glu 62 and a guanidine moiety appear to be critical for IL-2 inhibition by small molecules. By enforcing a particular geometry, hydrogen-bonding interactions set the register for the more malleable hydrophobic binding interactions and increase the likelihood that the compound will bind at only one site. Also, the addition of charged elements in the compound increase its solubility and decrease the likelihood of aggregation, precipitation, or denaturation.<sup>49,50</sup> From this perspective, the IL-2 binding site seems to be particularly well designed for small-molecule inhibitors. Nevertheless, the lessons learned through this small-molecule discovery effort should be generally applicable to other protein-protein targets.

## Conclusions

This report describes the evolution of a compound from millimolar affinity to nanomolar affinity. Often, the most difficult step in fragment assembly technology is advancing the molecules from the millimolar to micromolar stage. In the case of IL-2, this advancement was accomplished by linking two key binding elements with a chemically and structurally modular linker. The chemical series thus identified demonstrated attractive binding properties but reached an affinity plateau in the low micromolar range. This plateau was surpassed by incorporating fragments identified through Tethering. Using fragments in both the early and later stages of compound design efficiently improved compound potency and accessed new chemical space.

## Experimental Section

**General Methods.** <sup>1</sup>H NMR spectra were recorded on a Bruker 400 MHz spectrometer with chemical shifts reported in units of parts per million (ppm). Optical rotations were determined with a Jasco model P-1020 polarimeter. ESI mass spectra were obtained on a HP 1100MSD mass spectrometer. High-resolution mass spectra (HRMS) were determined on a

Applied Biosystems Qstar Pulsar-i. Flash column chromatography was performed using EM Science silica gel 60 (230–400 mesh). Elemental analyses were performed by Robertson Microlit Laboratories, Inc., Madison, NJ. Analytical thin layer chromatograms (TLCs) were run using glass thin layer plates coated with silica gel as supplied by E. Merck and were visualized by viewing under 254 nm UV or by exposure to a potassium permanganate solution in ethanol. Analytical HPLC was conducted on an Agilent 1100 LC/MS system using a C-18 Synergi Hydro-RP 4.6 mm  $\times$  150 mm (Phenomenex) at a flow rate of 1.5 mL per minute. The mobile phase consisted of water (A) and acetonitrile (B) each containing 0.1% trifluoroacetic acid by volume. Two methods were employed to assess the purity of compounds. In Method I, the gradient began at 5% B and ramped linearly to 100% B over 25 min. In Method II, the mobile phase was kept isocratic at 35% B for 24 min and then ramped up to 100% B over 1 min. UV absorbance was monitored at 220 nm and 254 nm. Preparative reverse phase high-pressure liquid chromatography (RP-HPLC) was carried out on a Gilson HPLC fitted with a Waters Nova-Pak C-18 (25  $\times$  100 mm) column eluting at 25 mL/min employing a gradient of acetonitrile:water (each containing 0.1% TFA) over 10 min and holding at 100% water for 3 min. Solvents and reagents were obtained from Aldrich Chemical Co., Lancaster, Nova Biochem, Fluka, Bionet, or Advanced ChemTech and used as received unless otherwise stated.

**(S)-2-(2-Methoxy-acetylamino)-3-(4-phenylethynyl-phenyl)-propionic Acid (2).** To a mixture of (S)-2-amino-3-(4-phenylethynyl-phenyl)-propionic acid methyl ester hydrochloride<sup>31</sup> (**4**, 90 mg, 0.285 mmol) and pyridine (140  $\mu$ L, 1.73 mmol) in dichloromethane (1.0 mL) was added methoxyacetyl chloride (58  $\mu$ L, 0.626 mmol) dropwise. After 3 h at ambient temperature, the reaction was diluted with ethyl acetate and washed sequentially with 1 N HCl (2 $\times$ ), saturated sodium bicarbonate (2 $\times$ ), and brine (2 $\times$ ). The organic layer was dried (Na<sub>2</sub>SO<sub>4</sub>) and concentrated. The crude residue was purified by flash column chromatography (SiO<sub>2</sub>: gradient 0 to 60% ethyl acetate in hexane) to yield 70 mg (70%) of a film. <sup>1</sup>H NMR (400 MHz, CDCl<sub>3</sub>)  $\delta$  7.52 (m, 2 H), 7.46 (d, 2 H, *J* = 8.0 Hz), 7.35 (m, 3 H), 7.12 (d, 2 H, *J* = 8.0 Hz), 6.96 (d, 1 H, *J* = 8.2 Hz), 4.93 (m, 1 H), 3.89 (s, 2 H), 3.72 (s, 3 H), 3.37 (s, 3 H), 3.18 (dd, 1 H, *J*<sub>1</sub> = 14.1 Hz, *J*<sub>2</sub> = 5.9 Hz), 3.10 (dd, 1 H, *J*<sub>1</sub> = 14.0 Hz, *J*<sub>2</sub> = 5.9 Hz); TLC (SiO<sub>2</sub>: 50% ethyl acetate in hexane): *R*<sub>f</sub> = 0.18; ES (+) MS *m/e* = 352 (M + 1).

To a solution containing the amide (53 mg, 0.150 mmol) in THF (0.84 mL) was added aqueous LiOH (0.80 M, 0.56 mL, 0.45 mmol). The reaction was stirred for 3 h followed by the addition of diethyl ether (3.0 mL) and saturated sodium bicarbonate. The layers were separated, and the organic phase was extracted with 2.0 mL saturated sodium bicarbonate. The combined aqueous layers were acidified with concentrated HCl and extracted with dichloromethane four times. The organic phases were combined, dried (MgSO<sub>4</sub>), and concentrated. The crude product was purified by reverse phase HPLC. The fractions containing pure compound were combined and concentrated. The residue was lyophilized to yield 10.9 mg (22%) of **2** a white powder. <sup>1</sup>H NMR (400 MHz, CDCl<sub>3</sub>)  $\delta$  7.49 (m, 4 H), 7.33 (m, 3 H), 7.17 (d, 2 H, *J* = 7.9 Hz), 7.01 (d, 1 H, *J* = 8.0 Hz), 4.93 (app q, 1 H, *J* = 6.5 Hz), 3.91 (s, 2 H), 3.36 (s, 3 H), 3.27 (dd, 1 H, *J*<sub>1</sub> = 14.1 Hz, *J*<sub>2</sub> = 5.4 Hz), 3.16 (dd, 1 H, *J*<sub>1</sub> = 14.0 Hz, *J*<sub>2</sub> = 6.5 Hz); TLC (SiO<sub>2</sub>: 2% AcOH and 8% MeOH in CHCl<sub>3</sub>): *R*<sub>f</sub> = 0.15; Anal. (C<sub>20</sub>H<sub>19</sub>NO<sub>4</sub>) C, H, N.

**(S)-2-(2-Amino-acetylamino)-3-(4-phenylethynyl-phenyl)-propionic Acid Methyl Ester Hydrochloride (5).** To a solution of **4** (0.25 g, 0.8 mmol) in dichloromethane (6 mL) were added *N*-Boc-glycine (0.18 g, 1.0 mmol), EDC (0.19 g, 1.0 mmol), HOBt (0.15 g, 1.0 mmol), and triethylamine (0.28 mL, 2.0 mmol). The mixture was stirred overnight and then was partitioned between dichloromethane and water. The aqueous layer was washed with dichloromethane (2 $\times$ ), and the organic layer was washed with 1 N HCl and saturated NaHCO<sub>3</sub>. The organic layer was dried over Na<sub>2</sub>SO<sub>4</sub>, filtered, and concentrated in vacuo to provide the desired amide. The crude residue was dissolved in HCl/dioxane (4.0 N, 5 mL), stirred for 45 min, and

then concentrated in vacuo to afford 350 mg (over theory) of a solid.  $^1\text{H NMR}$  (400 MHz,  $\text{CD}_3\text{OD}$ )  $\delta$  7.5 (m, 4 H), 7.37 (m, 3 H), 7.2 (m, 2H), 4.8 (m, 1 H), 3.7 (s, 3 H), 3.6 (m, 2 H), 3.3 (m, 1 H), 3.15 (m, 1 H); ES (+) MS  $m/e$  = 338 (M + 1).

**(2S)-[2-((2R)-Amino-propionylamino)-acetyl-amino]-3-(4-phenylethynyl-phenyl)-propionic Acid Methyl Hydrochloride (6c).** To a solution of **5** (0.1 g, 0.27 mmol) in dichloromethane (2 mL) were added *N*-Boc-D-alanine (66 mg, 0.35 mmol), EDC (67 mg, 0.35 mmol), HOBt (53 mg, 0.35 mmol), and triethylamine (0.1 mL, 0.7 mmol). The mixture was stirred overnight and then was partitioned between dichloromethane and water. The aqueous layer was washed with dichloromethane, and the organic layer was washed with 1 M HCl and saturated  $\text{NaHCO}_3$ . The organic layer was dried over  $\text{Na}_2\text{SO}_4$ , filtered, and concentrated in vacuo. The crude residue was dissolved in HCl/dioxane (4.0 N, 5 mL), stirred for 30 min, and then concentrated in vacuo to provide 120 mg (100%) of the corresponding amine hydrochloride salt.

**(2S)-[2-((2R)-Guanidino-propionylamino)-acetyl-amino]-3-(4-phenylethynyl-phenyl)-propionic Acid Methyl Ester Trifluoroacetate (7c).** To a solution of **6c** (75 mg, 0.17 mmol) in MeOH (2.5 mL) were added *tert*-butoxycarbonyliminopyrazol-1-yl-methyl-carbamic acid *tert*-butyl ester (77 mg, 0.25 mmol) and triethylamine (45  $\mu\text{L}$ , 0.32 mmol). The mixture was stirred overnight and then was partitioned between dichloromethane and water. The aqueous layer was washed with dichloromethane (2 $\times$ ), and the organic layer was washed with 1 N HCl, dried over  $\text{Na}_2\text{SO}_4$ , filtered, and concentrated in vacuo. The residue was dissolved in dichloromethane (1.5 mL) and TFA (1.5 mL) was added. The solution was stirred for 2 h and then concentrated to an oil. Purification by RP HPLC followed by lyophilization yielded **7c** (46 mg, 48%) as a white solid.  $^1\text{H NMR}$  (400 MHz,  $\text{CD}_3\text{OD}$ )  $\delta$  8.45 (d,  $J$  = 7.5, 1 H), 8.34 (m, 1 H), 7.61 (d,  $J$  = 7.4, 1 H), 7.47 (m, 4 H), 7.35 (m, 3 H), 7.23 (d,  $J$  = 7.9, 2 H), 4.74 (m, 1 H), 4.2 (m, 1 H), 3.9 (m, 2 H), 3.8 (s, 3H), 3.19 (dd,  $J$  = 13.8,  $J$  = 5.5, 1 H), 3.01 (dd,  $J$  = 13.7, 8.4, 1 H), 1.44 (d,  $J$  = 6.9, 3 H); ES (+) MS  $m/e$  = 450 (M + 1); Anal. ( $\text{C}_{24}\text{H}_{27}\text{N}_5\text{O}_4 \cdot 1.6\text{CF}_3\text{CO}_2\text{H}$ ) C, H, N.

**(S)-2-[2-(2-Guanidino-acetyl-amino)-acetyl-amino]-3-(4-phenylethynyl-phenyl)-propionic Acid Methyl Ester Trifluoroacetate (7a).** Following the procedures described for the synthesis of **7c** but using *N*-Boc-glycine in place of *N*-Boc-D-alanine, **7a** was prepared as a white powder.  $^1\text{H NMR}$  (400 MHz,  $\text{CD}_3\text{OD}$ )  $\delta$  7.5 (m, 4 H), 7.3 (m, 3 H), 7.17 (m, 1 H), 4.73 (m, 1 H), 3.95 (s, 2 H), 3.9 (m, 2 H), 3.8 (s, 3 H), 3.20 (dd,  $J$  = 13.5,  $J$  = 5.4, 1 H), 3.01 (dd,  $J$  = 13.8, 8.7, 1 H). ES (+) MS  $m/e$  = 436 (M + 1); HRMS (TOF) calcd for  $\text{C}_{23}\text{H}_{26}\text{N}_5\text{O}_4$  (M + H) $^+$  436.1985, found 436.1974. HPLC: Purity  $\geq$  98%.

**(2S)-[2-((2S)-Guanidino-propionylamino)-acetyl-amino]-3-(4-phenylethynyl-phenyl)-propionic Acid Methyl Ester Trifluoroacetate (7b).** Following the procedures described for the synthesis of **7c** but using *N*-Boc-alanine in place of *N*-Boc-D-alanine, **7b** was prepared as a white powder.  $^1\text{H NMR}$  (400 MHz,  $\text{CD}_3\text{OD}$ )  $\delta$  8.44 (d,  $J$  = 7.9, 1 H), 8.33 (m, 1 H), 7.61 (d,  $J$  = 7.5, 1 H), 7.47 (m, 4 H), 7.35 (m, 3 H), 7.23 (d,  $J$  = 7.9, 2 H), 4.75 (m, 1 H), 4.15 (m, 1 H), 4.0 (m, 1 H), 3.9 (m, 1 H), 3.8 (s, 3 H), 3.19 (dd,  $J$  = 13.8,  $J$  = 5.2, 1 H), 3.0 (dd,  $J$  = 13.8, 8.9, 1 H), 1.44 (d,  $J$  = 6.9, 3 H). ES (+) MS  $m/e$  = 450 (M + 1); Anal. ( $\text{C}_{24}\text{H}_{27}\text{N}_5\text{O}_4 \cdot 1.5\text{CF}_3\text{CO}_2\text{H}$ ) C, H, N.

**(2S)-[2-[2-(*N*-Methyl-guanidino)-acetyl-amino]-acetyl-amino]-3-(4-phenylethynyl-phenyl)-propionic Acid Methyl Ester (7d).** Following the procedures described for the synthesis of **7c** but using *N*-Boc-sarcosine in place of *N*-Boc-D-alanine, **7d** was prepared as a white powder. ES (+) MS  $m/e$  = 450 (M + 1).

**(2S)-[2S-[(1-Carbamimidoyl-pyrrolidine-2-carbonyl)-amino]-acetyl-amino]-3-(4-phenylethynyl-phenyl)-propionic Acid Methyl Ester Trifluoroacetate (7e).** Following the procedures described for the synthesis of **7c** but using *N*-Boc-proline in place of *N*-Boc-D-alanine, **7e** was prepared as a white powder. ES (+) MS  $m/e$  = 476 (M + 1).

**(2S)-[2S-[(1-Carbamimidoyl-pyrrolidine-2-carbonyl)-amino]-acetyl-amino]-3-(4-phenylethynyl-phenyl)-propionic Acid Methyl Ester Trifluoroacetate (7f).** Following

the procedures described for the synthesis of **7c** but using *N*-Boc-D-proline in place of *N*-Boc-D-alanine, **7f** was prepared as a white powder.  $^1\text{H NMR}$  (400 MHz,  $\text{CD}_3\text{OD}$ )  $\delta$  8.43 (d,  $J$  = 7.8, 2 H), 7.42–7.49 (m, 3 H), 7.22 (d,  $J$  = 7.9, 2 H), 4.72 (dd,  $J$  = 8.0, 5.6, 1 H), 4.47 (d,  $J$  = 6.4, 1 H), 3.96 (d,  $J$  = 16.8, 1 H), 3.84 (d,  $J$  = 16.8, 1 H), 3.59 (s, 3 H), 3.46–3.49 (m, 1 H), 3.42–3.45 (m, 1 H), 3.18 (dd,  $J$  = 13.7, 5.5, 1 H), 3.00 (dd,  $J$  = 13.7, 8.3, 1 H), 2.32–2.38 (m, 1 H), 2.16–2.24 (m, 1 H), 1.93–2.07 (m, 2 H). ES (+) MS  $m/e$  = 476 (M + 1).

**2S-[(2R)-(2-Guanidino-3-methyl-butyrylamino)-acetyl-amino]-3-(4-phenylethynyl-phenyl)-propionic Acid Methyl Ester Trifluoroacetate (7g).** Following the procedures described for the synthesis of **7c** but using *N*-Boc-D-valine in place of *N*-Boc-D-alanine, **7g** was prepared as a white powder.  $^1\text{H NMR}$  (400 MHz,  $\text{CD}_3\text{OD}$ )  $\delta$  7.20–7.55 (m, 9 H), 4.72 (dq,  $J$  = 7.8, 5.5, 1 H), 3.90–4.00 (m, 3 H), 3.73 (s, 3 H), 3.19 (dd,  $J$  = 13.8, 5.3, 1 H), 3.01 (dd,  $J$  = 8.5, 5.2, 1 H), 2.20–2.25 (m,  $J$  = 12.8, 6.5, 1 H), 0.82 (d,  $J$  = 6.7, 3 H), (0.74 (d,  $J$  = 6.7, 3 H). ES (+) MS  $m/e$  = 478 (M + 1).

**2S-[(2S)-(2-Guanidino-3-methyl-butyrylamino)-acetyl-amino]-3-(4-phenylethynyl-phenyl)-propionic Acid Methyl Ester Trifluoroacetate (7h).** Following the procedures described for the synthesis of **7c** but using *N*-Boc-valine in place of *N*-Boc-D-alanine, **7h** was prepared as a white powder. ES (+) MS  $m/e$  = 478 (M + 1).

**2S-[2-((2R)-3-Cyclohexyl-2-guanidino-propionylamino)-acetyl-amino]-3-(4-phenylethynyl-phenyl)-propionic Acid Methyl Ester Trifluoroacetate (7i).** Following the procedures described for the synthesis of **7c** but using *N*-Boc-D-cyclohexylalanine in place of *N*-Boc-D-alanine, **7i** was prepared as a white powder. ES (+) MS  $m/e$  = 532 (M + 1).

**(2S)-[2-((2R)-Cyclohexyl-2-guanidino-acetyl-amino)-acetyl-amino]-3-(4-phenylethynyl-phenyl)-propionic Acid Methyl Ester Trifluoroacetate (7j).** Following the procedures described for the synthesis of **7c** but using *N*-Boc-D-cyclohexylglycine in place of *N*-Boc-D-alanine, **7j** was prepared as a white powder.  $^1\text{H NMR}$  (400 MHz,  $\text{CD}_3\text{OD}$ )  $\delta$  8.4 (d,  $J$  = 7.7, 1 H), 8.28 (m, 1 H), 7.49 (m, 4 H), 7.35 (m, 3 H), 7.23 (d,  $J$  = 7.9, 2 H), 4.72 (m, 1 H), 3.9 (m, 3 H), 3.7 (s, 3 H), 3.19 (dd,  $J$  = 13.8,  $J$  = 5.3, 1 H), 3.01 (dd,  $J$  = 13.7, 8.3, 1 H), 1.75 (m, 6 H), 1.2 (m, 5 H). ES (+) MS  $m/e$  = 518 (M + 1).

**2S-[2-((2R)-2-Guanidino-3-methyl-pentanoylamino)-acetyl-amino]-3-(4-phenylethynyl-phenyl)-propionic Acid Methyl Ester Trifluoroacetate (7k).** Following the procedures described for the synthesis of **7c** but using *N*-Boc-D-leucine in place of *N*-Boc-D-alanine, **7k** was prepared as a white powder.  $^1\text{H NMR}$  (400 MHz,  $\text{CD}_3\text{OD}$ )  $\delta$  8.41 (d,  $J$  = 7.7, 1 H), 8.31 (s, 1 H), 7.47–7.49 (m, 2 H), 7.44 (d,  $J$  = 7.8, 2 H), 7.36–7.43 (m, 3 H), 7.23 (d,  $J$  = 7.0, 2 H), 4.71–4.75 (m, 1 H), 3.85–3.96 (m, 3 H), 3.73 (s, 3 H), 3.19 (dd,  $J$  = 13.8, 5.4, 1 H), 3.02 (dd,  $J$  = 13.8, 8.3, 1 H), 1.93–1.97 (m, 1 H), 1.48–1.55 (m, 1 H), 1.12–1.22 (m, 1 H), 0.77–0.94 (m, 6 H). ES (+) MS  $m/e$  = 492 (M + 1).

**2S-[2-((2R)-2-Guanidino-4,4-dimethyl-pentanoylamino)-acetyl-amino]-3-(4-phenylethynyl-phenyl)-propionic Acid Methyl Ester Trifluoroacetate (7l).** Following the procedures described for the synthesis of **7c** but using *N*-Boc-D-*tert*-butylalanine in place of *N*-Boc-D-alanine, **7l** was prepared as a white powder. ES (+) MS  $m/e$  = 506 (M + 1).

**2S-[2-((2R)-4-Carbamoyl-2-guanidino-butyrylamino)-acetyl-amino]-3-(4-phenylethynyl-phenyl)-propionic Acid Methyl Ester Trifluoroacetate (7m).** Following the procedures described for the synthesis of **7c** but using *N*-Boc-D-glutamine in place of *N*-Boc-D-alanine, **7m** was prepared as a white powder. ES (+) MS  $m/e$  = 507 (M + 1).

**(R)-(2-*tert*-Butoxycarbonylamino-2-cyclohexyl-acetyl-amino)-acetic Acid Pentafluorophenyl Ester (8).** To *N*-Boc-D-cyclohexylglycine (10.0 g, 38.9 mmol) in dichloromethane (100 mL) were added EDC (8.2 g, 42.8 mmol), HOBt monohydrate (6.5 g, 42.8 mmol) and triethylamine (11.9 mL, 85.5 mmol). Glycine methyl ester hydrochloride (5.8 g, 46.6 mmol) was added, and the reaction mixture was stirred overnight at room temperature. The mixture was diluted with dichloromethane (60 mL) and partitioned with water (70 mL).

The organic layer was separated, and the aqueous layer was extracted with dichloromethane (2 × 60 mL). The combined organic layer was washed with 1 N HCl (60 mL) and saturated NaHCO<sub>3</sub> (60 mL) and dried over Na<sub>2</sub>SO<sub>4</sub>. The solvent was evaporated, and the residue was dissolved in THF/water (3:1, 150 mL). To the resulting solution was then added lithium hydroxide (2.0 g, 83.5 mmol). The reaction mixture was stirred at room-temperature overnight and then acidified using 1 N HCl (100 mL). The mixture was extracted with ethyl acetate (3 × 100 mL), and the combined organic extracts were dried over Na<sub>2</sub>SO<sub>4</sub> and concentrated in vacuo. The residue was dissolved in THF (120 mL), and to the resulting solution was added pyridine (2.8 mL, 34.0 mmol) followed by pentafluorophenyl trifluoroacetate (5.8 mL, 34.0 mmol). The reaction mixture was stirred at room temperature for 2 h, and then the solvent was removed under reduced pressure. The residue was dissolved in ethyl acetate (100 mL) and was washed with 1 N HCl (70 mL) and saturated NaHCO<sub>3</sub> (70 mL). The organic layer was dried over Na<sub>2</sub>SO<sub>4</sub> and concentrated in vacuo to afford 13.5 g (72%) of **8**. <sup>1</sup>H NMR (400 MHz, CDCl<sub>3</sub>) δ 6.67 (br s, 1 H), 5.00 (br s, 1 H), 4.41 (m, 2 H), 3.98 (m, 1 H), 1.73–1.64 (m, 6 H), 1.43 (s, 9 H), 1.28–0.98 (m, 5 H). ES (+) MS *m/e* = 425 (M – 55).

**(R)-2-Cyclohexyl-N-(2-{4-[5-(2,4-dichloro-phenyl)-2H-pyrazol-3-yl]-piperidin-1-yl}-2-oxo-ethyl)-2-guanidinoacetamide (15a). General Library Protocol.** To 4-[5-(2,4-dichloro-phenyl)-2H-pyrazol-3-yl]-piperidine (44 mg, 0.15 mmol) in CH<sub>2</sub>Cl<sub>2</sub> (1 mL) was added ester **8** (96 mg, 0.20 mmol). The reaction was stirred at room temperature for 3 h, and then the solvent was removed under reduced pressure to yield the desired amide, which was used without purification.

The resulting amide was dissolved in HCl (1 mL, 4 M in 1,4-dioxane) and stirred at room temperature for 30 min. The solvent was removed under reduced pressure to provide 80 mg of the amine hydrochloride salt.

To the amine HCl salt (80 mg, 0.15 mmol) in MeOH (1 mL) and triethylamine (62 μL, 0.45 mmol) was added *N,N*-bis-Boc-1-guanylpyrazole (71 mg, 0.23 mmol). The reaction mixture was stirred at room-temperature overnight. The solvent was removed under reduced pressure to yield the bis-Boc-protected guanidine which was used without purification.

The protected guanidine (110 mg, 0.15 mmol) was dissolved in TFA/CH<sub>2</sub>Cl<sub>2</sub> (1 mL, 1:1) and stirred at room temperature for 3 h. The solvent was removed under reduced pressure to afford the desired product as the trifluoroacetate salt, which was purified via reverse-phase HPLC to provide **15a** as a white powder (12 mg, 12% over four steps). <sup>1</sup>H NMR (400 MHz, CD<sub>3</sub>OD) δ 7.64–7.54 (m, 2 H), 7.40 (m, 1 H), 6.56 (s, 1 H), 4.59 (d, 1 H, *J* = 13.4 Hz), 4.32–3.97 (m, 4 H), 3.32 (m, 1 H), 3.07 (m, 1 H), 2.88 (m, 1 H), 2.13–1.62 (m, 10 H), 1.36–1.11 (m, 5 H). Anal. (C<sub>25</sub>H<sub>33</sub>Cl<sub>2</sub>N<sub>7</sub>O<sub>2</sub>·1.5CF<sub>3</sub>CO<sub>2</sub>H) C, H, N.

**4-(2-Methoxycarbonyl-acetyl)-piperidine-1-carboxylic Acid *tert*-Butyl Ester (10).** To a solution of 4-acetyl-piperidine-1-carboxylic acid *tert*-butyl ester<sup>51</sup> (**9**, 25 g, 110 mmol) in THF (435 mL) at –78 °C was added dropwise lithium bis(trimethylsilyl)amide (1.0 M in THF, 220 mL, 220 mmol). To the resulting mixture was added methyl cyanofornate (15.7 mL, 198 mmol). After 30 min at –78 °C, the reaction was warmed to room temperature, diluted with diethyl ether, and then quenched with water. The mixture was extracted with water, 0.5 N aqueous HCl, and brine. The organic layer was dried over Na<sub>2</sub>SO<sub>4</sub> and concentrated to yield 33.4 g (over theory) of a colorless oil. A pure sample of **10** was obtained by flash column chromatography (SiO<sub>2</sub>: gradient 0 to 40% ethyl acetate in hexane). <sup>1</sup>H NMR (400 MHz, CDCl<sub>3</sub>) δ 4.10 (br s, 2 H), 3.73 (s, 3 H), 3.50 (s, 2 H), 2.77 (m, 2 H), 2.60 (m, 1 H), 1.83 (m, 2 H), 1.57 (m, 2 H), 1.44 (s, 9 H); TLC (SiO<sub>2</sub>: 50% ethyl acetate in hexane): *R<sub>f</sub>* = 0.34; ES (+) MS *m/e* = 286 (M + 1).

**4-(5-Oxo-4,5-dihydro-1H-pyrazol-3-yl)-piperidine-1-carboxylic Acid *tert*-Butyl Ester (11).** A mixture of the keto-ester **10** (32.8 g) obtained in the previous step and hydrazine hydrate (5.58 mL, 115 mmol) in ethanol (120 mL) was heated at 70 °C until TLC indicated complete consumption of the

starting material (~1 h). The reaction mixture was cooled to ambient temperature, and the resulting precipitate (11.5 g) was collected by filtration. The filtrate was concentrated, redissolved in hot ethanol, and allowed to reach room temperature. After standing for several hours, a second crop (4.3 g) was collected and when combined provided 15.8 g (54% from **9**) of an off-white solid. <sup>1</sup>H NMR (400 MHz, CD<sub>3</sub>OD) δ 4.11 (m, 2 H), 3.30 (m, 1 H), 2.86 (br s, 2 H), 2.73 (m, 2 H), 1.88 (m, 2 H), 1.53 (m, 2 H), 1.46 (s, 9 H); TLC (SiO<sub>2</sub>: 10% methanol in dichloromethane): *R<sub>f</sub>* = 0.27; ES (+) MS *m/e* = 268 (M + 1).

**4-(1-*tert*-Butoxycarbonyl-5-trifluoromethanesulfonyloxy-1H-pyrazol-3-yl)-piperidine-1-carboxylic acid *tert*-butyl Ester (12).** (Regiochemistry of Boc-addition not determined.) A solution of **11** (11.5 g, 43.0 mmol) and *N*-phenyltrifluoromethanesulfonimide (19.9 g, 55.9 mmol) in anhydrous dichloromethane (150 mL) under nitrogen at 0 °C was treated with triethylamine (60 mL, 430 mmol). The mixture was allowed to reach ambient temperature. After 1 h, LC-MS indicated complete consumption of **11**, and the solvent was removed under reduced pressure. Purification of the crude residue by flash column chromatography (SiO<sub>2</sub>: gradient 0 to 40% ethyl acetate in hexane) yielded 14.8 g (86%) of a white solid. <sup>1</sup>H NMR (400 MHz, CDCl<sub>3</sub>) δ 5.95 (s, 1 H), 4.13 (br s, 2 H), 2.82 (m, 3 H), 1.94 (m, 2 H), 1.61 (m, 2 H), 1.46 (s, 9 H); TLC (SiO<sub>2</sub>: 50% ethyl acetate in hexane): *R<sub>f</sub>* = 0.45; ES (+) MS *m/e* = 400 (M + 1).

To a solution of the triflate (14.8 g, 36.9 mmol) in dichloromethane (35 mL) were added a mixture of di-*tert*-butyl dicarbonate (12.1 g, 55.6 mmol), DMAP (0.45 g, 3.71 mmol), and triethylamine (75 mL) in dichloromethane (70 mL). After 1 h, HPLC indicated complete conversion to the protected material. The solvent was removed under reduced pressure, and the crude residue was purified by flash column chromatography (SiO<sub>2</sub>: gradient 0 to 10% ethyl acetate in hexane) to yield 16.9 g (91%) **12** as a white solid. <sup>1</sup>H NMR (400 MHz, CDCl<sub>3</sub>) δ 6.08 (s, 1 H), 4.23 (br s, 2 H), 3.47 (m, 1 H), 2.81 (m, 2 H), 2.00 (m, 2 H), 1.64 (s, 9 H), 1.49 (m, 2 H), 1.47 (s, 9 H); TLC (SiO<sub>2</sub>: 20% ethyl acetate in hexane): *R<sub>f</sub>* = 0.36; ES (+) MS *m/e* = 522 (M + 23). HRMS (TOF): exact mass calcd for C<sub>10</sub>H<sub>13</sub>F<sub>3</sub>N<sub>3</sub>O<sub>5</sub>S (M – *t*-Bu – Boc + H)<sup>+</sup> 344.0528, found 344.0579. Anal. (C<sub>19</sub>H<sub>28</sub>F<sub>3</sub>N<sub>3</sub>O<sub>7</sub>S) C, H, N.

**4-[5-(2,3-Dichloro-phenyl)-2H-pyrazol-3-yl]-piperidine-1-carboxylic acid *tert*-butyl Ester (13e). Suzuki Couplings with 12. General Procedure A.** A mixture of **12** (300 mg, 0.601 mmol), 2,3-dichlorophenylboronic acid (143 mg, 0.75 mmol), Pd(PPh<sub>3</sub>)<sub>4</sub> (69 mg, 0.0601 mmol), and aqueous potassium carbonate (2 M, 0.90 mL, 1.80 mmol) in dioxane (2.1 mL) was heated at 102–103 °C (oil bath temperature) in a sealed vial. After 3 h, the mixture was cooled to room temperature, and the phases were separated. The organic layer was dried (Na<sub>2</sub>SO<sub>4</sub>), filtered through a plug of Celite, and concentrated. The crude residue was purified by flash column chromatography (SiO<sub>2</sub>: 0 to 50% ethyl acetate in hexane) to yield 106 mg (45%) of **13e** as a white powder. <sup>1</sup>H NMR (400 MHz, CDCl<sub>3</sub>) δ 7.51 (d, 1 H, *J* = 7.8 Hz), 7.47 (dd, 1 H, *J*<sub>1</sub> = 8.0 Hz, *J*<sub>2</sub> = 1.4 Hz), 7.23 (app t, 1 H, *J* = 7.9 Hz), 6.50 (s, 1 H), 4.21 (br s, 2 H), 2.86 (m, 3 H), 2.02 (d, 2 H, *J* = 11.4 Hz), 1.69 (app q, 2 H, *J* = 11.4 Hz), 1.50 (s, 9 H); TLC (SiO<sub>2</sub>: 50% ethyl acetate in hexane): *R<sub>f</sub>* = 0.27; ES (+) MS *m/e* = 418 (M + 23). HRMS (TOF): exact mass calcd for C<sub>15</sub>H<sub>16</sub>Cl<sub>2</sub>N<sub>3</sub>O<sub>2</sub> (M – *t*-Bu + H)<sup>+</sup> 340.0620, found 340.0646.

**4-[5-(2,3-Dichloro-phenyl)-2H-pyrazol-3-yl]-piperidine Hydrochloride (14e). Deprotection of *N*-Boc Piperidine Derivatives. General Procedure B.** To a solution of **13e** (90 mg, 0.227 mmol) in dichloromethane (0.5 mL) was added 4 N HCl in dioxane (4.0 mL). The mixture was stirred at ambient temperature for 2 h and was then diluted with diethyl ether (4.0 mL). The resulting white precipitate was collected by filtration, washed with diethyl ether (3 × 4 mL), and dried under high-vacuum to yield 48 mg (72%) of a white powder. <sup>1</sup>H NMR (400 MHz, DMSO-*d*<sub>6</sub>) δ 9.18 (br s, 1 H), 8.95 (br s, 1 H), 7.66 (m, 2 H), 7.42 (app t, 1 H, *J* = 7.9 Hz), 6.55 (s, 1 H), 3.31 (d, 2 H, *J* = 12.4 Hz), 3.02 (m, 3 H), 2.14 (d, 2 H, *J*

= 12.7 Hz), 1.86 (q, 2 H,  $J = 11.8$  Hz); HRMS (TOF): exact mass calcd for  $C_{14}H_{16}Cl_2N_3$  ( $M + H$ )<sup>+</sup> 296.0721, found 296.0746.

**(R)-[Cyclohexyl-(2-{4-[5-(2,3-dichloro-phenyl)-2H-pyrazol-3-yl]-piperidin-1-yl}-2-oxo-ethyl-carbamoyl)-methyl]-carbamic Acid *tert*-Butyl Ester. Acylation of 4-Aryl Piperidine Derivatives. General Procedure C.** To a mixture of **14e** (50 mg, 0.150 mmol) and triethylamine (0.5 mL) in dichloromethane (2.0 mL) was added 72 mg (0.150 mmol) of **8**. The resulting solution was stirred at ambient temperature until LC/MS indicated complete conversion to product. The solvent was then removed under reduced pressure to yield a crude residue that was used directly in the following step. ES (+) MS  $m/e = 592$  ( $M + 1$ ).

**(R)-2-Cyclohexyl-*N*-(2-{4-[5-(2,3-dichloro-phenyl)-2H-pyrazol-3-yl]-piperidin-1-yl}-2-oxo-ethyl)-2-guanidino-acetamide Trifluoroacetate (15e). Deprotection/Guanidinylation/Deprotection Sequence. General Procedure D.** The crude residue obtained in the previous step (~0.150 mmol of **28**) was dissolved in HCl (4.0 N in dioxane, 1 mL) and was stirred at room temperature for 1 h. The mixture was concentrated in vacuo, and the residual crude amine hydrochloride salt was taken up in methanol (2.0 mL). To the resulting solution was added triethylamine (0.5 mL) followed by *N,N*-bis-Boc-1-guanylpyrazole (62 mg, 0.20 mmol). The reaction mixture was stirred at room-temperature overnight. The solvent was removed under reduced pressure, and the residue was treated with TFA/dichloromethane (1:1, 1 mL) at room temperature. When LC/MS indicated complete deprotection, the mixture was concentrated to yield a crude product that was purified by RP HPLC. The fractions containing pure compound were combined and concentrated. The residue was lyophilized under high-vacuum to yield 24 mg (25% from **14e**) of **15e** as a white powder. <sup>1</sup>H NMR (400 MHz, CD<sub>3</sub>OD)  $\delta$  7.56 (d, 1 H,  $J = 1.5$  Hz), 7.52 (d, 1 H,  $J = 1.5$  Hz), 7.38 (t, 1 H,  $J = 8.0$  Hz), 6.52 (s, 1 H), 4.57 (d, 1 H,  $J = 14.15$  Hz), 4.33–3.93 (m, 4 H), 3.26 (t, 1 H,  $J = 13.6$ ), 3.06 (app t, 1 H,  $J = 11.8$  Hz), 2.87 (app t, 1 H,  $J = 12.6$  Hz), 2.08 (app t, 2 H,  $J = 14.8$  Hz), 1.85–1.63 (m, 8 H), 1.36–1.09 (m, 5 H). Anal. (C<sub>25</sub>H<sub>33</sub>-Cl<sub>2</sub>N<sub>7</sub>O<sub>2</sub>·1.2CF<sub>3</sub>CO<sub>2</sub>H) C, H, N.

**(R)-2-Cyclohexyl-2-guanidino-*N*-(2-oxo-2-[4-(5-phenyl)-2H-pyrazol-3-yl]-piperidin-1-yl)-ethyl}-acetamide Trifluoroacetate (15b).** The title compound was prepared from **12** according to General Procedures A–D using phenylboronic acid instead of 2,3-dichlorophenylboronic acid. White powder (10 mg, 2.9% from **12**). <sup>1</sup>H NMR (400 MHz, CD<sub>3</sub>OD)  $\delta$  7.72 (m, 2 H), 7.50–7.33 (m, 3 H), 6.53 (s, 1 H), 4.59 (d, 1 H,  $J = 12.1$  Hz), 4.34–3.99 (m, 4 H), 3.28 (m, 1 H), 3.04 (m, 1 H), 2.89 (m, 1 H), 2.06–2.12 (m, 2 H), 1.68–1.93 (m, 8 H), 1.14–1.37 (m, 5 H). Anal. (C<sub>25</sub>H<sub>35</sub>N<sub>7</sub>O<sub>2</sub>·2.35CF<sub>3</sub>CO<sub>2</sub>H) C, H, N.

**(R)-*N*-(2-{4-[5-(2-Chloro-phenyl)-2H-pyrazol-3-yl]-piperidin-1-yl}-2-oxo-ethyl)-2-cyclohexyl-2-guanidino-acetamide Trifluoroacetate (15c).** The title compound was prepared from **12** according to General Procedures A–D using 2-chlorophenylboronic acid instead of 2,3-dichlorophenylboronic acid. White powder (11 mg, 3% from **12**). <sup>1</sup>H NMR (400 MHz, CD<sub>3</sub>OD)  $\delta$  7.59 (m, 1 H), 7.51 (m, 1 H), 7.38 (m, 2 H), 6.57 (s, 1 H), 4.60 (m, 1 H), 4.39–3.95 (m, 4 H), 3.33 (m, 1 H), 3.07 (m, 1 H), 2.87 (m, 1 H), 2.11 (m, 2 H) 1.99–1.60 (m, 8 H), 1.37–1.13 (m, 5 H). HRMS (TOF) calcd for C<sub>25</sub>H<sub>35</sub>ClN<sub>7</sub>O<sub>2</sub> ( $M + H$ )<sup>+</sup> 500.2541, found 500.2558. HPLC: Purity  $\geq 98\%$ .

**(R)-*N*-(2-{4-[5-(3-Chloro-phenyl)-2H-pyrazol-3-yl]-piperidin-1-yl}-2-oxo-ethyl)-2-cyclohexyl-2-guanidino-acetamide Trifluoroacetate (15d).** The title compound was prepared from **12** according to General Procedures A–D using 3-chlorophenylboronic acid instead of 2,3-dichlorophenylboronic acid. White powder (15 mg, 4.1% from **12**). <sup>1</sup>H NMR (400 MHz, CD<sub>3</sub>OD)  $\delta$  7.78–7.67 (m, 2 H), 7.50–7.33 (m, 2 H), 6.57 (s, 1 H), 4.58 (m, 1 H), 4.34–4.00 (m, 4 H), 3.32 (m, 1 H), 3.05 (m, 1 H), 2.89 (m, 1 H), 2.09–1.71 (m, 10 H), 1.36–1.11 (m, 5 H). Anal. (C<sub>25</sub>H<sub>34</sub>ClN<sub>7</sub>O<sub>2</sub>·1.8CF<sub>3</sub>CO<sub>2</sub>H) C, H, N.

**(R)-2-Cyclohexyl-*N*-(2-{4-[5-(3,4-dichloro-phenyl)-2H-pyrazol-3-yl]-piperidin-1-yl}-2-oxo-ethyl)-2-guanidino-acetamide Trifluoroacetate (15f).** The title compound was prepared from **12** according to General Procedures A–D using

3,4-dichlorophenylboronic acid instead of 2,3-dichlorophenylboronic acid. <sup>1</sup>H NMR (400 MHz, CD<sub>3</sub>OD)  $\delta$  7.68 (d, 1 H,  $J = 8.3$  Hz), 7.58–7.49 (m, 2 H), 6.58 (s, 1 H), 4.59 (d, 1 H,  $J = 13.2$  Hz), 4.35–3.96 (m, 4 H), 3.28 (t, 1 H,  $J = 13.2$  Hz), 3.05 (t, 1 H,  $J = 11.0$  Hz), 2.88 (t, 1 H,  $J = 12.2$  Hz), 2.13–1.67 (m, 10 H), 1.37–1.10 (m, 5 H). ES (+) MS  $m/e = 536$  ( $M + 1$ ).

**(R)-2-Cyclohexyl-2-guanidino-*N*-(2-oxo-2-[4-(5-*o*-tolyl)-2H-pyrazol-3-yl]-piperidin-1-yl)-ethyl}-acetamide Trifluoroacetate (15g).** The title compound was prepared from **12** according to General Procedures A–D using *o*-tolylboronic acid (100 mg, 0.20 mmol) instead of 2,3-dichlorophenylboronic acid. White powder (19.1 mg, 16% from **12**). <sup>1</sup>H NMR (400 MHz, CD<sub>3</sub>OD)  $\delta$  7.49 (d, 1 H,  $J = 8.3$  Hz), 7.38 (d, 1 H,  $J = 6.8$  Hz), 7.29 (m, 2 H), 7.24 (m, 1 H), 6.37 (s, 1 H), 4.58 (d, 1 H,  $J = 13.3$  Hz), 4.40–4.03 (m, 2 H), 4.00 (br s, 2 H), 3.25 (app t, 1 H,  $J = 13.2$  Hz), 3.07 (m, 1 H), 2.87 (app t, 1 H,  $J = 12.4$ ), 2.37 (s, 3 H), 2.09 (app t, 2 H,  $J = 14.0$  Hz), 1.90–1.68 (m, 8 H), 1.34–1.11 (m, 5 H); Anal. (C<sub>26</sub>H<sub>37</sub>N<sub>7</sub>O<sub>2</sub>·1.5CF<sub>3</sub>CO<sub>2</sub>H) C, H, N.

**(R)-2-Cyclohexyl-2-guanidino-*N*-(2-oxo-2-[4-(5-*m*-tolyl)-2H-pyrazol-3-yl]-piperidin-1-yl)-ethyl}-acetamide (15h).** The title compound was prepared from **12** according to General Procedures A–D using *m*-tolylboronic acid instead of 2,3-dichlorophenylboronic acid. White powder (10 mg, 2.8% from **12**). <sup>1</sup>H NMR (400 MHz, CD<sub>3</sub>OD)  $\delta$  7.50–7.56 (m, 3 H), 7.31 (t, 1 H,  $J = 7.7$  Hz), 7.18 (d, 1 H,  $J = 7.3$  Hz), 6.52 (s, 1 H), 4.61 (m, 1 H), 3.98–4.38 (m, 4 H), 3.31 (m, 1 H), 3.04 (m, 1 H), 2.89 (m, 1 H), 2.40 (s, 3 H), 2.09 (m, 2 H), 1.67–1.84 (m, 8 H), 1.14–1.37 (m, 5 H). Anal. (C<sub>26</sub>H<sub>37</sub>N<sub>7</sub>O<sub>2</sub>·2.5CF<sub>3</sub>CO<sub>2</sub>H) C, H, N.

**(R)-2-Cyclohexyl-*N*-(2-{4-[5-(2,3-dimethyl-phenyl)-2H-pyrazol-3-yl]-piperidin-1-yl}-2-oxo-ethyl)-2-guanidino-acetamide Trifluoroacetate (15i).** The title compound was prepared from **12** according to General Procedures A–D using 2,3-dimethylphenylboronic acid instead of 2,3-dichlorophenylboronic acid. <sup>1</sup>H NMR (400 MHz, CD<sub>3</sub>OD)  $\delta$  7.22–7.12 (m, 3 H), 6.25 (s, 1 H), 4.59 (d, 1 H,  $J = 13.2$  Hz), 4.34–3.96 (m, 4 H), 3.28 (t, 1 H,  $J = 13.2$  Hz), 3.10–3.02 (m, 1 H), 2.89 (t, 1 H,  $J = 13.2$  Hz), 2.34 (s, 3 H), 2.26 (s, 3 H), 2.14–1.67 (m, 10 H), 1.36–1.11 (m, 5 H). ES (+) MS  $m/e = 494$  ( $M + 1$ ).

**(R)-*N*-(2-{4-[5-(2-Chloro-4-hydroxy-phenyl)-2H-pyrazol-3-yl]-piperidin-1-yl}-2-oxo-ethyl)-2-cyclohexyl-2-guanidino-acetamide Trifluoroacetate (15j).** The title compound was prepared from **12** according to General Procedures A–D using 2-chloro-4-hydroxyphenylboronic acid instead of 2,3-dichlorophenylboronic acid. ES (+) MS  $m/e = 517$  ( $M + 1$ ).

**(R)-*N*-(2-{4-[5-(2-Chloro-4-methoxy-phenyl)-2H-pyrazol-3-yl]-piperidin-1-yl}-2-oxo-ethyl)-2-cyclohexyl-2-guanidino-acetamide Trifluoroacetate (15k).** The title compound was prepared from **12** according to General Procedures A–D using 2-chloro-4-methoxyphenylboronic acid instead of 2,3-dichlorophenylboronic acid. ES (+) MS  $m/e = 531$  ( $M + 1$ ).

**4-[5-(2,3-Dichlorophenyl)-1-methyl-1H-pyrazol-3-yl]-piperidine-1-carboxylic Acid *tert*-Butyl Ester (16a) and 4-[5-(2,3-Dichlorophenyl)-2-methyl-2H-pyrazol-3-yl]-piperidine-1-carboxylic Acid *tert*-Butyl Ester (16b).** To a solution of 4-acetyl-piperidine-1-carboxylic acid *tert*-butyl ester<sup>51</sup> (**9**, 1.8 g, 8.0 mmol) in 1,2-dimethoxyethane (30 mL) at –78 °C under nitrogen was added dropwise lithium bis(trimethylsilyl)amide (1.0 M in THF, 16 mL, 16 mmol). The reaction was warmed to room temperature, stirred for 30 min, and then cooled again to –78 °C. To the mixture was added methyl 2,3-dichlorobenzoate (2.0 g, 9.5 mmol), and the resulting solution was refluxed overnight. The reaction mixture was cooled to room temperature, treated with 1.0 M HCl (15 mL), and extracted with ethyl acetate (3 × 30 mL). The combined organic extracts were dried over Na<sub>2</sub>SO<sub>4</sub> and concentrated to yield 3.6 g an amber oil. Purification of the crude material by flash column chromatography (SiO<sub>2</sub>: 20% ethyl acetate in hexanes) provided 1.5 g (48%) of the diketone intermediate.

To a solution of the diketone (300 mg, 0.75 mmol) in methanol (3 mL) was added methylhydrazine (80  $\mu$ L, 1.5 mmol). The resulting mixture was stirred for 1 h at 50 °C and then concentrated under reduced pressure. Purification of the

residue by flash chromatography (SiO<sub>2</sub>: 10 to 40% ethyl acetate in hexanes) provided 81 mg (26%) of regioisomer **16a** and 23 mg (7%) of regioisomer **16b**. **Major regioisomer (16a)**: <sup>1</sup>H NMR (400 MHz, DMSO-*d*<sub>6</sub>) δ 7.77 (dd, 1 H, *J*<sub>1</sub> = 7.6 Hz, *J*<sub>2</sub> = 1.9 Hz), 7.50–7.43 (m, 2 H), 6.24 (s, 1 H), 3.97 (br s, 2 H), 3.57 (s, 3 H), 2.92–2.76 (m, 3 H), 1.90 (d, 2 H, *J* = 11.1 Hz), 1.47 (app qd, 2 H, *J*<sub>1</sub> = 12.0 Hz, *J*<sub>2</sub> = 3.3 Hz), 1.41 (s, 9 H). ES (+) MS *m/e* = 410 (M + 1). Anal. (C<sub>20</sub>H<sub>25</sub>Cl<sub>2</sub>N<sub>3</sub>O<sub>2</sub>) C, H, N. **Minor regioisomer (16b)**: <sup>1</sup>H NMR (400 MHz, DMSO-*d*<sub>6</sub>) δ 7.69 (dd, 1 H, *J*<sub>1</sub> = 7.8 Hz, *J*<sub>2</sub> = 1.6 Hz), 7.60 (dd, 1 H, *J*<sub>1</sub> = 8.0 Hz, *J*<sub>2</sub> = 1.5 Hz), 7.38 (app t, 1 H, *J* = 7.9 Hz), 6.58 (s, 1 H), 4.17 (br s, 2 H), 3.83 (s, 3 H), 2.94–2.78 (m, 3 H), 1.89 (d, 2 H, *J* = 10.8 Hz), 1.43 (m, 2 H), 1.42 (s, 9 H). ES (+) MS *m/e* = 410 (M + 1). Anal. (C<sub>20</sub>H<sub>25</sub>Cl<sub>2</sub>N<sub>3</sub>O<sub>2</sub>) C, H, N.

**(R)-2-Cyclohexyl-N-(2-{4-[5-(2,3-dichloro-phenyl)-2-methyl-2H-pyrazol-3-yl]-piperidin-1-yl}-2-oxo-ethyl)-2-guanidino-acetamide Trifluoroacetate (22)**. The title compound was prepared according to General Procedures B–D but using **16a** (62 mg, 0.15 mmol) instead of **13e**. White powder (11 mg, 10% from **16a**). <sup>1</sup>H NMR (400 MHz, CD<sub>3</sub>OD) δ 7.60–7.50 (m, 2 H), 7.34 (t, 1 H, *J* = 7.9 Hz), 6.53 (s, 1 H), 4.65 (d, 1 H, *J* = 13.7 Hz), 4.35–3.89 (m, 7 H), 3.31 (m, 1 H), 3.13 (m, 1 H), 2.88 (m, 1 H), 2.07 (m, 2 H), 1.92–1.57 (m, 8 H), 1.47–1.11 (m, 5 H). HRMS (TOF) calcd for C<sub>26</sub>H<sub>36</sub>Cl<sub>2</sub>N<sub>7</sub>O<sub>2</sub> (M + H)<sup>+</sup> 548.2308, found 548.2319. HPLC: Purity ≥98%.

**(R)-2-Cyclohexyl-N-(2-{4-[5-(2,3-dichloro-phenyl)-1-methyl-1H-pyrazol-3-yl]-piperidin-1-yl}-2-oxo-ethyl)-2-guanidino-acetamide Trifluoroacetate (23)**. The title compound was prepared according to General Procedures B–D but using **16b** (62 mg, 0.15 mmol) instead of **13e**. White powder (10 mg, 10% from **16b**). <sup>1</sup>H NMR (400 MHz, CD<sub>3</sub>OD) δ 7.71 (d, 1 H, *J* = 8.0 Hz), 7.47–7.36 (m, 2 H), 6.24 (s, 1 H), 4.58 (d, 1 H, *J* = 12.0 Hz), 4.33–4.06 (m, 2 H), 3.99 (m, 2 H), 3.65 (s, 3 H), 3.25 (m, 1 H), 3.02–2.87 (m, 2 H), 2.11–1.63 (m, 10 H), 1.37–1.14 (m, 5 H). HRMS (TOF) calcd for C<sub>26</sub>H<sub>36</sub>Cl<sub>2</sub>N<sub>7</sub>O<sub>2</sub> (M + H)<sup>+</sup> 548.2308, found 548.2318. HPLC: Purity ≥98%.

**4-[5-(2,3-Dichloro-phenyl)-4-methyl-2H-pyrazol-3-yl]-piperidine-1-carboxylic Acid *tert*-Butyl Ester (18)**. To a solution of 4-propionyl-piperidine-1-carboxylic acid *tert*-butyl ester **17** (0.37 g, 1.53 mmol) in DMF (5 mL) was added NaH (60% in mineral oil, 0.12 g, 3.07 mmol). The reaction was stirred for 15 min followed by addition of methyl 2,3-dichlorobenzoate (0.47 g, 2.3 mmol). After being stirred overnight, the reaction mixture was diluted with EtOAc and H<sub>2</sub>O. The layers were separated, and the aqueous layer was extracted with EtOAc. The organic layer was dried over MgSO<sub>4</sub> and concentrated under reduced pressure. The crude material was purified by flash chromatography (SiO<sub>2</sub>: 5% EtOAc in hexanes) to afford the diketone which was used directly in the next step.

To the diketone in EtOH (3 mL) was added hydrazine (0.5 mL). After 30 min, the reaction was concentrated under reduced pressure and purified by flash chromatography (SiO<sub>2</sub>: 33% EtOAc in hexanes) to afford **18**. ES (+) MS *m/e* = 411 (M + 1).

**(R)-2-Cyclohexyl-N-(2-{4-[5-(2,3-dichloro-phenyl)-4-methyl-2H-pyrazol-3-yl]-piperidin-1-yl}-2-oxo-ethyl)-2-guanidino-acetamide Trifluoroacetate (24)**. The title compound was prepared according to General Procedures B–D but using **18** instead of **13e**. ES (+) MS *m/e* = 549 (M + 1).

**4-[3-(2,4-Dichlorophenyl)-phenyl]-piperidine-1-carboxylic Acid *tert*-Butyl Ester (19)**. To 3-piperidin-4-yl phenol (2.0 g, 11.3 mmol) in dichloromethane (50 mL) was added triethylamine (1.7 mL, 12.4 mmol) followed by Boc-anhydride (2.7 g, 12.4 mmol). The reaction mixture was stirred at room temperature for 2 days and was then washed with 1 M HCl (1 × 35 mL). The organic layer was dried over Na<sub>2</sub>SO<sub>4</sub> and concentrated in vacuo to provide 3.4 g (>100%) of crude material that was used without further purification.

To the phenol (3.1 g, 11.3 mmol) in dichloromethane (50 mL) was added triethylamine (1.7 mL, 12.4 mmol) followed by *N*-phenyltrifluoromethanesulfonimide (4.4 g, 12.4 mmol). The reaction was stirred overnight at room temperature and was then washed sequentially with 1 M HCl (1 × 35 mL) and 1 M NaOH (1 × 35 mL). The organic layer was dried over Na<sub>2</sub>SO<sub>4</sub>,

concentrated under reduced pressure, and purified via flash chromatography (SiO<sub>2</sub>: 25% ethyl acetate in hexanes) to afford 3.1 g (67% after two steps) of the triflate as a clear oil.

To the triflate (300 mg, 0.73 mmol) and 2,4-dichlorophenylboronic acid (153 mg, 0.81 mmol) in 1,4-dioxane (3 mL) was added aqueous potassium carbonate (733 μL, 1.5 mmol, 2 M) followed by tetrakis(triphenylphosphine)palladium (30 mg, 0.026 mmol). The reaction mixture was refluxed overnight, diluted with ethyl acetate (8 mL), and washed with 1 M HCl (8 mL). The aqueous layer was extracted with ethyl acetate (2 × 8 mL), and the combined organic layer was washed with saturated NaHCO<sub>3</sub> solution, dried over Na<sub>2</sub>SO<sub>4</sub> and concentrated in vacuo. The resulting residue was purified via flash chromatography (SiO<sub>2</sub>: 25% ethyl acetate in hexanes) to afford 130 mg (44%) of **19**. <sup>1</sup>H NMR (400 MHz, CDCl<sub>3</sub>) δ 7.49 (s, 1H), 7.40–7.34 (m, 1H), 7.31–7.20 (m, 5H), 4.32–4.20 (m, 2H), 2.89–2.65 (m, 3H), 1.91–1.83 (m, 2H), 1.72–1.58 (m, 2H), 1.48 (s, 9H).

**25**. The title compound was prepared according to General Procedures B–D but using **19** instead of **13e**. <sup>1</sup>H NMR (400 MHz, CD<sub>3</sub>OD) δ 7.55 (br s, 1 H), 7.42–7.20 (m, 6 H), 4.64 (br s, 1 H), 4.35–3.92 (m, 4 H), 3.24 (br s 1 H), 2.96–2.72 (m, 2 H), 1.99–1.63 (m, 10 H), 1.37–1.07 (m, 5 H). ES (+) MS *m/e* = 544 (M + 1).

**4-[3-(2,4-Dichlorophenyl)-[1,2,4]oxadiazol-5-yl]-piperidine-1-carboxylic acid *tert*-Butyl Ester (21)**. To 2,4-dichlorobenzonitrile (200 mg, 1.2 mmol) in MeOH (5 mL) was added hydroxylamine (85 mg, 1.3 mmol, 50wt % in H<sub>2</sub>O). The reaction mixture was heated at 50 °C for 30 min and then refluxed for 1 h. The mixture was cooled to room temperature, and the solvent was removed under reduced pressure. The resulting residue was then dissolved in ethyl acetate (5 mL), washed with water (5 mL), dried over Na<sub>2</sub>SO<sub>4</sub>, and concentrated in vacuo to yield 272 mg (>100%) of **20** which was used without further purification.

To piperidine-1,4-dicarboxylic acid mono-*tert*-butyl ester (91 mg, 0.40 mmol) in *N,N*-dimethylformamide (1 mL) with diisopropylethylamine (83 μL, 0.48 mmol) was added tetrafluoroborohexafluorophosphate (116 mg, 0.44 mmol). The reaction was stirred at room temperature for 15 min, and then a solution of amidoxime **20** (90 mg, 0.44 mmol) in THF (1 mL) was added. The resulting mixture was stirred for 3 h at 110 °C and then was diluted with ethyl acetate (3 mL), washed with water (1 × 3 mL), and washed with 1 M HCl (1 × 3 mL). The organic layer was dried over Na<sub>2</sub>SO<sub>4</sub> and concentrated under reduced pressure to afford 205 mg of **21** which was used without further purification. ES (+) MS *m/e* = 341 (M – 56).

**(R)-2-Cyclohexyl-N-(2-{4-[3-(2,4-dichloro-phenyl)-[1,2,4]-oxadiazol-5-yl]-piperidin-1-yl}-2-oxo-ethyl)-2-guanidino-acetamide Trifluoroacetate (26)**. The title compound was prepared according to General Procedures B–D but using **21** (164 mg, 0.40 mmol) instead of **13e**. <sup>1</sup>H NMR (400 MHz, CD<sub>3</sub>OD) δ 7.94 (d, 1 H, *J* = 8.3 Hz), 7.71 (s, 1 H), 7.53 (d, 1 H, *J* = 8.3 Hz), 4.65 (s, 1 H), 4.32–3.95 (m, 4 H), 3.52–3.34 (m, 2 H), 3.01 (t, 1 H, *J* = 12.2 Hz), 2.25 (t, 2 H, *J* = 14.7 Hz), 1.87–1.70 (m, 8 H), 1.37–1.10 (m, 5 H). ES (+) MS *m/e* = 538 (M + 1).

**2,3-Dichloro-4-triisopropylsilyloxy-benzoyl Chloride (27)**. To a solution of 2,3-dichlorophenol (10.0 g, 61.3 mmol) in dichloromethane (50 mL) was added bromine (4.11 mL, 79.8 mmol) dropwise. After 2 h, HPLC indicated complete consumption of the starting material. The reaction mixture was slowly poured into a 10% aqueous sodium thiosulfate solution. The phases were separated, and the aqueous layer was extracted with dichloromethane (3×). The combined organic layers were dried over Na<sub>2</sub>SO<sub>4</sub> and concentrated. Purification of the crude residue by flash column chromatography (SiO<sub>2</sub>: 0 to 20% ethyl acetate in hexane) yielded 7.86 g, 53% of a white solid. Spectroscopic data is identical to that of commercially available 4-bromo-2,3-dichloro-phenol from Chem-Service Inc. <sup>1</sup>H NMR (400 MHz, CDCl<sub>3</sub>) δ 7.44 (d, 1 H, *J* = 8.9 Hz), 6.86 (d, 1 H, *J* = 8.9 Hz), 5.72 (s, 1 H); TLC (SiO<sub>2</sub>: 20% ethyl acetate in hexane): *R*<sub>f</sub> = 0.29.

To a solution of 4-bromo-2,3-dichloro-phenol (11.7 g, 48.4 mmol) in dry THF (100 mL) was added triethylamine (7.4 mL, 53.2 mmol) followed by triisopropylsilyl chloride (11.4 mL, 53.2 mmol). The reaction was stirred for 1 h at room temperature. Water (250 mL) and ethyl acetate (250 mL) were added and the layers separated. The aqueous layer was washed with additional ethyl acetate (200 mL). The organic layers were combined, dried over MgSO<sub>4</sub>, filtered through a short plug of silica gel, concentrated under reduced pressure, and dried under high vacuum at 50 °C for 48 h to yield 19.0 g (99%) of a viscous oil. <sup>1</sup>H NMR (400 MHz, CDCl<sub>3</sub>) δ 7.36 (d, 1 H, *J* = 8.9 Hz), 6.72 (d, 1 H, *J* = 8.9 Hz), 1.32–1.27 (m, 3 H), 1.10 (d, 18 H, *J* = 7.7 Hz). Anal. (C<sub>15</sub>H<sub>23</sub>BrCl<sub>2</sub>OSi) C, H, N.

To a –78 °C solution of the silyl ether (15.4 g, 38.7 mmol) in anhydrous THF (385 mL) under nitrogen was added *n*-butyllithium (1.57 M in hexane, 24.6 mL, 38.7 mmol) dropwise. After 10 min at –78 °C, carbon dioxide was bubbled through the solution for approximately 10 min. The mixture was allowed to reach room temperature and was quenched by careful addition of water (310 mL) followed by aqueous HCl (1.0 N, 38.7 mL, 38.7 mmol). The mixture was extracted with diethyl ether (3×), and the combined organic layer was dried over MgSO<sub>4</sub> and concentrated. Purification of the crude residue by flash column chromatography (SiO<sub>2</sub>: 0 to 70% ethyl acetate in hexane) yielded 6.65 g (47%) of the acid as a white solid. <sup>1</sup>H NMR (400 MHz, CDCl<sub>3</sub>) δ 7.88 (d, 1 H, *J* = 8.8 Hz), 6.89 (d, 1 H, *J* = 8.8 Hz), 1.32–1.27 (m, 3 H), 1.15 (d, 18 H, *J* = 7.4 Hz); TLC (SiO<sub>2</sub>: 30% ethyl acetate in hexane): *R*<sub>f</sub> = 0.39; ES (+) MS *m/e* = 363 (*M* + 1). Anal. (C<sub>16</sub>H<sub>24</sub>Cl<sub>2</sub>O<sub>3</sub>Si) C, H, N.

To a solution of the acid (6.45 g, 17.8 mmol) in anhydrous dichloromethane (120 mL) under nitrogen was added DMF (1.38 mL, 17.8 mmol) followed by dropwise addition of oxalyl chloride (2.01 mL, 23.1 mmol). After 10 min, HPLC indicated complete consumption of the starting material, and 1,2-dichloroethane was added. The solvent was removed in vacuo, and the excess oxalyl chloride was removed by coevaporation with 1,2-dichloroethane. The residue was dried under high vacuum and was then used without further purification.

**4-Ethynyl-piperidine-1-carboxylic Acid *tert*-Butyl Ester (29).** To a heterogeneous solution of 4-formyl-piperidine-1-carboxylic acid *tert*-butyl ester<sup>52</sup> (23.7 g, 0.11 mol) and potassium carbonate (30.7 g, 0.22 mol) in MeOH (1.0 L) was added dropwise dimethyl-1-diazo-2-oxopropylphosphonate<sup>53</sup> (28, 21.3 g, 0.11 mol) in MeOH (100 mL). The resulting mixture was stirred for 3 h and concentrated under reduced pressure. The residue was diluted with diethyl ether (500 mL) and 5% aqueous NaHCO<sub>3</sub> (700 mL). The layers were separated, and the aqueous layer was washed with diethyl ether (2 × 500 mL). The organic layer was dried over MgSO<sub>4</sub> and concentrated under reduced pressure to afford crude 29 (22.4 g, 96%). <sup>1</sup>H NMR (CDCl<sub>3</sub>) δ 3.67 (m, 2 H), 3.20–3.15 (m, 2 H), 2.58 (m, 1 H), 2.09 (s, 1 H), 1.77–1.75 (m, 2 H), 1.60–1.57 (m, 2 H), 1.45 (s, 9 H). ES (+) MS *m/e* = 154 (*M* – *t*-Bu + 2H)<sup>+</sup>.

**(R)-[1-[2-(4-Ethynyl-piperidin-1-yl)-2-oxo-ethylcarbamoyl]-3-methyl-butyl]-carbamic acid *tert*-Butyl Ester (30).** A solution of 24 (6.0 g, 28.7 mmol) in HCl/dioxane (4.0 N, 50 mL) was stirred at room temperature for 30 min. The solvent was removed under reduced pressure to afford the desired amine (4.2 g, 100%) as the hydrochloride salt.

To *N*-Boc-glycine (5.0 g, 28.7 mmol) in dichloromethane (120 mL) were added EDC (6.6 g, 34.4 mmol), HOBt monohydrate (4.6 g, 34.4 mmol), and triethylamine (9.6 mL, 68.8 mmol). The piperidine amine HCl salt (4.2 g, 28.7 mmol) was added, and the reaction was stirred at room-temperature overnight. The reaction mixture was partitioned with water (100 mL) and separated. The aqueous layer was extracted with dichloromethane (2 × 100 mL), and the combined organic layer was washed with 1 M HCl (100 mL) and saturated NaHCO<sub>3</sub> (100 mL) and dried over Na<sub>2</sub>SO<sub>4</sub> to provide the desired amide.

To the amide (7.7 g, 28.7 mmol) was added HCl/dioxane (4.0 N, 50 mL), and the reaction was stirred at room temperature for 30 min. The solvent was removed under reduced pressure to give the desired amine (5.8 g, 100%) as the hydrochloride salt.

To *N*-Boc-D-leucine (6.6 g, 28.7 mmol) in dichloromethane (120 mL) were added EDC (6.6 g, 34.4 mmol), HOBt monohydrate (4.6 g, 34.4 mmol), and triethylamine (9.6 mL, 68.9 mmol). To the activated acid solution was added the amine (5.8 g, 28.7 mmol), and the reaction was stirred at room temperature for 4 h. The reaction mixture was partitioned with water (100 mL) and separated. The aqueous layer was extracted with dichloromethane (2 × 100 mL), and the combined organic layer was washed with 1 M HCl (100 mL) and saturated NaHCO<sub>3</sub> (100 mL) and dried over Na<sub>2</sub>SO<sub>4</sub>. The solvent was removed under reduced pressure to provide the crude amide, and purification by flash chromatography (SiO<sub>2</sub>: 25% ethyl acetate in hexanes) provided 6.6 g (61% over four steps). <sup>1</sup>H NMR (400 MHz, CDCl<sub>3</sub>) δ 7.04 (br s, 1H), 4.91 (br s, 1H), 4.20 (br s, 1H), 4.04 (m, 2H), 3.08 (m, 1H), 3.56 (m, 2H), 3.28 (m, 1H), 2.73 (br s, 1H), 2.14 (s, 1H), 1.80 (m, 2H), 1.68 (m, 4H), 1.48 (m, 1H), 1.44 (s, 9H), 0.94 (m, 6H). ES (+) MS *m/e* = 324 (*M* – 55). Anal. (C<sub>20</sub>H<sub>33</sub>N<sub>3</sub>O<sub>4</sub>) C, H, N.

**(R)-[1-(2-[4-[5-(2,3-Dichloro-4-triisopropylsilyloxy-phenyl)-2-methyl-2H-pyrazol-3-yl]-piperidin-1-yl]-2-oxo-ethylcarbamoyl)-3-methyl-butyl]-carbamic Acid *tert*-Butyl Ester (31).** A round-bottom flask containing 27 (~17.8 mmol), CuI (0.17 g, 0.89 mmol), PdCl<sub>2</sub>(PPh<sub>3</sub>)<sub>2</sub> (0.63 mg, 0.89 mmol), and 30 (6.75 g, 17.8 mmol) was flushed with nitrogen for several minutes and then charged with a degassed solution of triethylamine (4.97 mL, 35.6 mmol) in toluene (120 mL). The reaction was monitored by HPLC, and the solvent was removed when 27 had been completely consumed. The crude residue was immediately used in the following step. ES (+) MS *m/e* = 724 (*M* + 1).

The crude material and methylhydrazine (9.47 mL, 178 mmol) in ethanol (120 mL) was stirred at ambient temperature for 1.5 h. The reaction mixture was concentrated and then redissolved in dichloromethane. The organic phase was washed with water, and the resulting aqueous layer was extracted with dichloromethane (2×). The combined organic layers were dried over Na<sub>2</sub>SO<sub>4</sub> and concentrated. The crude residue was purified by flash column chromatography (SiO<sub>2</sub>: 50 to 100% ethyl acetate in hexane) to yield 7.0 g (52%) of 31 as a single regioisomer. <sup>1</sup>H NMR (400 MHz, CDCl<sub>3</sub>) δ 7.47 (d, 1 H, *J* = 8.6 Hz), 7.09 (br s, 1 H), 6.84 (d, 1 H, *J* = 8.6 Hz), 6.43 (s, 1 H), 4.93 (br s, 1 H), 4.73 (d, 1 H, *J* = 12.1 Hz), 4.28–4.13 (m, 3 H), 3.88 (s, 3 H), 3.85 (m, 1 H), 3.17 (app t, 1 H, *J* = 11.9 Hz), 2.84 (m, 1 H), 2.77 (app t, 1 H, *J* = 12.9 Hz), 2.03 (m, 2 H), 1.66–1.59 (m, 4 H), 1.45 (m, 1 H), 1.43 (s, 9 H), 1.33 (m, 3 H), 1.12 (m, 18 H), 0.93 (m, 6 H); TLC (SiO<sub>2</sub>: ethyl acetate): *R*<sub>f</sub> = 0.19; ES (+) MS *m/e* = 752 (*M* + 1). Anal. (C<sub>37</sub>H<sub>59</sub>Cl<sub>2</sub>N<sub>5</sub>O<sub>5</sub>-Si) C, H, N.

**(R)-[1-(2-[4-[5-(2,3-Dichloro-4-hydroxy-phenyl)-2-methyl-2H-pyrazol-3-yl]-piperidin-1-yl]-2-oxo-ethylcarbamoyl)-3-methyl-butyl]-carbamic Acid *tert*-Butyl Ester (32).** To a 0 °C solution of 31 (7.0 g, 9.3 mmol) in anhydrous THF (50 mL) was added tetrabutylammonium fluoride (1.0 M in THF, 14 mL, 14 mmol) dropwise. The reaction mixture was stirred for 30 min and then partitioned between water (200 mL) and ethyl acetate (200 mL). The aqueous layer was washed with ethyl acetate (3 × 200 mL), and the combined organic layer was dried (MgSO<sub>4</sub>) and concentrated under reduced pressure. The crude residue was purified by flash column chromatography (SiO<sub>2</sub>: 0–10% methanol in dichloromethane) to yield 5.0 g (90%) of an off-white solid. <sup>1</sup>H NMR (400 MHz, CD<sub>3</sub>OD) δ 7.35 (d, 1 H, *J* = 8.5 Hz), 7.14 (d, 1 H, *J* = 8.8 Hz), 6.40 (s, 1 H), 4.61 (d, 1 H, *J* = 12.8 Hz), 4.16–4.05 (m, 4 H), 3.88 (s, 3 H), 3.25 (m, 1 H), 3.06 (m, 1 H), 2.83 (m, 1 H), 2.01 (m, 2 H), 1.71–1.53 (m, 6 H), 1.44 (s, 9 H), 2.83 (m, 6 H); TLC (SiO<sub>2</sub>: 5% methanol in dichloromethane): *R*<sub>f</sub> = 0.10; ES (+) MS *m/e* = 596 (*M* + 1). HRMS (TOF) calcd for C<sub>28</sub>H<sub>40</sub>Cl<sub>2</sub>N<sub>5</sub>O<sub>5</sub> (*M* + H)<sup>+</sup> 596.2406, found 596.2432. Anal. (C<sub>28</sub>H<sub>39</sub>Cl<sub>2</sub>N<sub>5</sub>O<sub>5</sub>) C, H, N.

**2R-Guanidino-4-methyl-pentanoic Acid (2-[4-[5-(2,3-dichloro-4-hydroxy-phenyl)-2-methyl-2H-pyrazol-3-yl]-piperidin-1-yl]-2-oxo-ethyl)-amide Trifluoroacetate (33b).** The title compound was prepared according to General Procedure D using 32. ES (+) MS *m/e* = 538 (*M* + 1).



**2,3-Dichloro-4-bromoanisole (34).** A mixture of 4-bromo-2,3-dichlorophenol (637 mg, 2.63 mmol), iodomethane (0.660 mL, 10.5 mmol), and  $\text{Cs}_2\text{CO}_3$  (1.72 g, 5.26 mmol) in DMF (8.0 mL) was stirred at 70 °C for 3 h. After being cooled to ambient temperature, the mixture was diluted with water and extracted with dichloromethane (3 $\times$ ). The combined organic phases were washed with brine, dried ( $\text{MgSO}_4$ ), and concentrated. Purification by flash chromatography ( $\text{SiO}_2$ : 5% EtOAc in hexanes) provided **34** as a white solid (520 mg, 77%).  $^1\text{H}$  NMR (400 MHz,  $\text{CDCl}_3$ )  $\delta$  7.49 (d, 1 H,  $J = 9.0$  Hz), 6.75 (d, 1 H,  $J = 9.0$  Hz), 3.90 (s, 3 H); TLC ( $\text{SiO}_2$ : 5% EtOAc in hexanes):  $R_f = 0.35$ .

**2,3-Dichloro-4-methoxy-benzoic Acid (35).** Following the procedure described for the synthesis of **27** but using **34** (400 mg, 1.56 mmol) in place of 4-bromo-2,3-dichloro-1-triisopropylsilyloxybenzene, **35** was prepared as a white powder (280 mg, 81%).  $^1\text{H}$  NMR (400 MHz,  $\text{CDCl}_3$ )  $\delta$  8.00 (d, 1 H,  $J = 8.9$  Hz), 6.92 (d, 1 H,  $J = 8.9$  Hz), 3.99 (s, 3 H); TLC ( $\text{SiO}_2$ : 2% AcOH and 50% ethyl acetate in hexanes):  $R_f = 0.21$ .

**(R)-[1-(2-{4-[5-(2,3-Dichloro-4-methoxy-phenyl)-2-methyl-2H-pyrazol-3-yl]-piperidin-1-yl]-2-oxo-ethylcarbamoyl}-3-methyl-butyl)-carbamic Acid tert-Butyl Ester (36).** Following the procedures described for the synthesis of **27** and **31** but using **35** (140 mg, 1.56 mmol), **36** was prepared as a tan solid.  $^1\text{H}$  NMR (400 MHz,  $\text{CD}_3\text{OD}$ )  $\delta$  7.52 (d, 1 H,  $J = 8.7$  Hz), 7.11 (d, 1 H,  $J = 8.8$  Hz), 6.45 (s, 1 H), 4.64 (d, 1 H,  $J = 12.9$  Hz), 4.18–3.99 (m, 4 H), 3.95 (s, 3 H), 3.91 (s, 3 H), 3.28 (app t, 1 H,  $J = 12.8$  Hz), 3.10 (m, 1 H), 2.85 (app t,  $J = 11.8$  Hz), 2.04 (m, 2 H), 1.73 (m, 2 H), 1.59 (m, 3 H), 1.46 (s, 9 H), 0.98 (d, 3 H,  $J = 7.0$  Hz), 0.96 (d, 3 H,  $J = 7.1$  Hz). TLC ( $\text{SiO}_2$ : 5% MeOH in dichloromethane):  $R_f = 0.13$ ; ES (+) MS  $m/e = 610$  (M + 1). HRMS (TOF) calcd for  $\text{C}_{24}\text{H}_{34}\text{Cl}_2\text{N}_5\text{O}_3$  (M - Boc + H) $^+$  510.2039, found 510.2103.

**(R)-2-Guanidino-4-methyl-pentanoic Acid (2-{4-[5-(2,3-dichloro-4-methoxy-phenyl)-2-methyl-2H-pyrazol-3-yl]-piperidin-1-yl}-2-oxo-ethyl)-amide Trifluoroacetate (33c).** The title compound was prepared according to General Procedure D using **36**. White powder, 13.6 mg (3.2% overall from **35**).  $^1\text{H}$  NMR (400 MHz,  $\text{CD}_3\text{OD}$ )  $\delta$  7.51 (d, 1 H,  $J = 8.7$  Hz), 7.09 (d, 1 H,  $J = 8.8$  Hz), 6.42 (s, 1 H), 4.61 (d, 1 H,  $J = 12.9$  Hz), 4.30–3.97 (m, 4 H), 3.93 (s, 3 H), 3.89 (s, 3 H), 3.30 (m, 1 H), 3.07 (m, 1 H), 2.84 (m, 1 H), 2.03 (app t, 2 H,  $J = 13.9$  Hz), 1.76–1.68 (m, 4 H), 1.51 (m, 1 H), 0.99 (m, 6 H); Anal. ( $\text{C}_{25}\text{H}_{35}\text{Cl}_2\text{N}_7\text{O}_3 \cdot 1.5\text{CF}_3\text{CO}_2\text{H}$ ) C, H, N.

**3-Chloromethyl-benzoic Acid Allyl Ester (37).** To a mixture of 3-(chloromethyl)benzoic acid (1.00 g, 5.85 mmol), EDC (1.80 g, 9.40 mmol), and DMAP (75 mg, 0.61 mmol) in dichloromethane (20 mL) was added allyl alcohol (600  $\mu\text{L}$ , 8.82 mmol). After 2 h at ambient temperature, LC/MS indicated complete conversion. The solution was concentrated and taken up in ethyl acetate. The mixture was washed with aqueous 1 N HCl (3 $\times$ ), aqueous sat.  $\text{NaHCO}_3$  (1 $\times$ ), and brine (1 $\times$ ). The organic phase was dried ( $\text{MgSO}_4$ ) and concentrated to yield 796 mg (64%) of a colorless liquid.  $^1\text{H}$  NMR (400 MHz,  $\text{CDCl}_3$ )  $\delta$  8.06 (s, 1 H), 8.00 (d, 1 H,  $J = 7.8$  Hz), 7.57 (d, 1 H,  $J = 7.6$  Hz), 7.43 (app t, 1 H,  $J = 7.7$  Hz), 6.03 (m, 1 H), 5.40 (d, 1 H,  $J = 17.2$  Hz), 5.28 (d, 1 H,  $J = 10.4$  Hz), 4.81 (dd, 2 H,  $J_1 = 5.6$  Hz,  $J_2 = 0.8$  Hz), 4.60 (s, 2 H); ES (+) MS  $m/e = 211$  (M + 1).

**(R)-3-[4-(5-{1-[2-(2-tert-Butoxycarbonylamino-4-methyl-pentanoylamino)-acetyl]-piperidin-4-yl]-1-methyl-1H-pyrazol-3-yl)-2,3-dichloro-phenoxy-methyl]-benzoic Acid Allyl Ester (38).** General Alkylation Procedure E. A mixture of **32** (700 mg, 1.17 mmol), **37** (247 mg, 1.17 mmol), and  $\text{Cs}_2\text{CO}_3$  (762 mg, 2.34 mmol) in DMF (7.0 mL) was stirred at 70 °C for 3 h. After being cooled to ambient temperature, the mixture was diluted with water and extracted with dichloromethane (3 $\times$ ). The combined organic phases were washed with brine, dried ( $\text{MgSO}_4$ ), and concentrated. The crude residue was purified by flash column chromatography ( $\text{SiO}_2$ : 0 to 5% methanol in dichloromethane) to yield 807 mg (90%) of a white foam.  $^1\text{H}$  NMR (400 MHz,  $\text{CDCl}_3$ )  $\delta$  8.10 (s, 1 H), 7.99 (d, 1 H,  $J = 7.7$  Hz), 7.65 (d, 1 H,  $J = 7.5$  Hz), 7.53 (d, 1 H,  $J = 8.7$  Hz), 7.43 (app t, 1 H,  $J = 7.7$  Hz), 7.14 (br s, 1 H),

6.88 (d, 1 H,  $J = 8.8$  Hz), 6.39 (s, 1 H), 6.00 (m, 1 H), 5.37 (dd, 1 H,  $J_1 = 17.2$  Hz,  $J_2 = 1.3$  Hz), 5.25 (d, 1 H,  $J = 10.4$  Hz), 5.17 (s, 2 H), 5.10 (br s, 1 H), 4.78 (m, 2 H), 4.66 (d, 1 H,  $J = 12.0$  Hz), 4.18 (br s, 1 H), 4.06 (m, 2 H), 3.90 (br s, 1 H), 3.83 (s, 3 H), 3.13 (app t, 1 H,  $J = 12.0$  Hz), 2.86 (m, 1 H), 2.73 (app t, 1 H,  $J = 12.9$  Hz), 1.99 (app t, 2 H,  $J = 9.9$  Hz), 1.63–1.50 (m, 4 H), 1.46 (m, 1 H), 1.40 (s, 9 H), 0.90 (m, 6 H); TLC ( $\text{SiO}_2$ : 5% methanol in dichloromethane):  $R_f = 0.25$ ; ES (+) MS  $m/e = 770$  (M + 1).

**(R)-3-[4-(5-{1-[2-(2-tert-Butoxycarbonylamino-4-methyl-pentanoylamino)-acetyl]-piperidin-4-yl]-1-methyl-1H-pyrazol-3-yl)-2,3-dichloro-phenoxy-methyl]-benzoic Acid (39).** To a solution of **38** (719 mg, 0.933 mmol) and Pd( $\text{PPh}_3$ ) $_4$  (54.0 mg, 0.0466 mmol) in THF (4.0 mL) under nitrogen was added morpholine (407  $\mu\text{L}$ , 4.66 mmol). The resulting mixture was stirred at ambient temperature for 1 h. The solvent was then removed in vacuo, and the crude residue was purified by flash column chromatography (0.5% AcOH and 0–5% methanol in dichloromethane) to yield 577 mg (85%) of a tan solid.  $^1\text{H}$  NMR (400 MHz,  $\text{CDCl}_3$ )  $\delta$  9.31 (br s, 1 H), 8.13 (s, 1 H), 8.02 (d, 1 H,  $J = 7.7$  Hz), 7.66 (d, 1 H,  $J = 7.6$  Hz), 7.54 (d, 1 H,  $J = 8.7$  Hz), 7.44 (app t, 1 H,  $J = 7.6$  Hz), 7.13 (d, 1 H,  $J = 7.1$  Hz), 6.89 (d, 1 H,  $J = 8.9$  Hz), 6.39 (s, 1 H), 5.32 (br s, 1 H), 5.16 (s, 2 H), 4.70 (d, 1 H,  $J = 12.1$  Hz), 4.28–4.13 (m, 3 H), 3.88 (m, 1 H), 3.85 (s, 3 H), 3.15 (app t, 1 H,  $J = 12.1$  Hz), 2.84 (m, 1 H), 2.78 (app t, 1 H,  $J = 12.9$  Hz), 1.99 (m, 2 H), 1.66–1.41 (m, 5 H), 1.40 (s, 9 H), 0.91 (m, 6 H); TLC ( $\text{SiO}_2$ : 0.5% AcOH 5% methanol in dichloromethane):  $R_f = 0.18$ ; ES (+) MS  $m/e = 730$  (M + 1). Anal. ( $\text{C}_{36}\text{H}_{45}\text{Cl}_2\text{N}_5\text{O}_7$ ) C, H, N.

**(R)-3-[2,3-Dichloro-4-(5-{1-[2-(2-guanidino-4-methyl-pentanoylamino)-acetyl]-piperidin-4-yl]-1-methyl-1H-pyrazol-3-yl)-phenoxy-methyl]-benzoic Acid Trifluoroacetate (33g).** The title compound was prepared according to General Procedure D using **39** (120 mg, 0.164 mmol). White powder, 30.2 mg (23% from **39**).  $^1\text{H}$  NMR (400 MHz,  $\text{CD}_3\text{OD}$ )  $\delta$  8.15 (s, 1 H), 7.99 (d, 1 H,  $J = 7.7$  Hz), 7.72 (d, 1 H,  $J = 7.6$  Hz), 7.52–7.47 (m, 2 H), 7.15 (d, 1 H,  $J = 8.8$  Hz), 6.41 (s, 1 H), 5.28 (s, 2 H), 4.62 (d, 1 H,  $J = 13.0$  Hz), 4.30–4.01 (m, 2 H), 3.88 (s, 3 H), 3.27 (m, 1 H), 3.07 (m, 1 H), 2.84 (m, 1 H), 1.99 (app t, 2 H,  $J = 14.2$  Hz), 1.76–1.68 (m, 4 H), 1.51 (m, 1 H), 0.98 (m, 6 H); Anal. ( $\text{C}_{32}\text{H}_{39}\text{Cl}_2\text{N}_7\text{O}_5 \cdot \text{CF}_3\text{CO}_2\text{H}$ ) C, H, N.

**(R)-2-Guanidino-4-methyl-pentanoic Acid (2-{4-[5-(4-benzyloxy-2,3-dichloro-phenyl)-2-methyl-2H-pyrazol-3-yl]-piperidin-1-yl}-2-oxo-ethyl)-amide (33d).** The title compound was prepared from **31** according to General Procedures D and E using benzylbromide in place of **37**. White powder (4 mg, 4.5% from **32**).  $^1\text{H}$  NMR (400 MHz,  $\text{CD}_3\text{OD}$ )  $\delta$  7.69–7.33 (m, 6 H), 7.17 (d, 1 H,  $J = 8.8$  Hz), 6.45 (s, 1 H), 5.36 (s, 2 H), 4.66 (d, 1 H,  $J = 13.2$  Hz), 4.33–4.00 (m, 4 H), 3.91 (s, 3 H), 3.28 (m, 1 H), 3.12 (m, 1 H), 2.87 (m, 1 H), 2.06 (m, 2 H), 1.75–1.55 (m, 5 H), 1.03–0.99 (m, 6 H). Anal. ( $\text{C}_{31}\text{H}_{39}\text{Cl}_2\text{N}_7\text{O}_3 \cdot 2\text{CF}_3\text{CO}_2\text{H}$ ) C, H, N.

**(R)-3-[4-(5-{1-[2-(2-tert-Butoxycarbonylamino-4-methyl-pentanoylamino)-acetyl]-piperidin-4-yl]-1-methyl-1H-pyrazol-3-yl)-2,3-dichloro-phenoxy-methyl]-benzoic Acid Methyl Ester (40).** The title compound was prepared according to General Procedure E using **32** (75 mg, 0.120 mmol), 4-bromomethyl-benzoic acid methyl ester (43 mg, 0.190 mmol), and  $\text{K}_2\text{CO}_3$  (35 mg, 0.250 mmol) in DMF (0.5 mL). The crude product (76 mg, 85%) was used without further purification. ES (+) MS  $m/e = 744$  (M + H).

**(R)-4-[2,3-Dichloro-4-(5-{1-[2-(2-guanidino-4-methyl-pentanoylamino)-acetyl]-piperidin-4-yl]-1-methyl-1H-pyrazol-3-yl)-phenoxy-methyl]-benzoic Acid Methyl Ester Trifluoroacetate (33e).** The title compound was prepared according to General Procedure D using **40** (76 mg, 0.10 mmol). White powder, 4 mg (4.9% overall from **40**).  $^1\text{H}$  NMR (400 MHz,  $\text{CDCl}_3$ )  $\delta$  8.07 (d, 2 H,  $J = 8.3$  Hz), 7.63 (d, 2 H,  $J = 8.3$  Hz), 7.51 (d, 1 H,  $J = 8.7$  Hz), 7.17 (d, 1 H,  $J = 8.8$  Hz), 6.46 (s, 1 H), 5.34 (s, 2 H), 4.65 (d, 1 H,  $J = 13.2$  Hz), 4.29–4.02 (m, 4 H), 3.93 (s, 3 H), 3.91 (s, 3 H), 3.30 (m, 1 H), 3.30–3.10 (m, 2 H), 2.88 (m, 1 H), 2.06 (m, 1 H) 1.78–1.71 (m, 4 H), 1.50 (m, 1

H), 1.01 (m, 6 H). HRMS (TOF) calcd for  $C_{33}H_{42}Cl_2N_7O_5$  ( $M + H$ )<sup>+</sup> 686.2624, found 686.2614. HPLC: Purity  $\geq 98\%$ .

**(R)-4-[4-(5-{1-[2-(2-*tert*-Butoxycarbonylamino-4-methyl-pentanoylamino)-acetyl]-piperidin-4-yl}-1-methyl-1*H*-pyrazol-3-yl)-2,3-dichloro-phenoxy-methyl]-benzoic Acid (41).** To a solution of **40** (75 mg, 0.12 mmol) in THF (0.5 mL) was added aqueous LiOH (1 M, 2.0 mL, 2.0 mmol). The resulting mixture was heated at 60 °C for 18 h. The reaction mixture was cooled, concentrated under reduced pressure, and purified by RP HPLC to afford 36 mg (39%) of a film. ES (+) MS  $m/e = 730$  ( $M + 1$ ).

**(R)-4-[2,3-Dichloro-4-(5-{1-[2-(2-guanidino-4-methyl-pentanoylamino)-acetyl]-piperidin-4-yl}-1-methyl-1*H*-pyrazol-3-yl)-phenoxy-methyl]-benzoic Acid Trifluoroacetate (33f).** The title compound was prepared according to General Procedure D using **41** (36 mg, 0.05 mmol). White powder, 4 mg (12% from **41**). <sup>1</sup>H NMR (400 MHz, CDCl<sub>3</sub>)  $\delta$  8.07 (d, 2 H,  $J = 8.2$  Hz), 7.62 (d, 2 H,  $J = 8.1$  Hz), 7.51 (d, 1 H,  $J = 8.7$  Hz), 7.18 (d, 1 H,  $J = 8.9$  Hz), 6.46 (s, 1 H), 5.35 (s, 1 H), 4.21–4.00 (m, 4 H), 3.92 (s, 3 H), 3.15 (m, 1 H), 2.88 (m, 1 H), 2.07 (m, 2 H), 1.75–1.55 (m, 6 H), 1.03–0.99 (m, 6 H). HRMS (TOF) calcd for  $C_{32}H_{40}Cl_2N_7O_5$  ( $M + H$ )<sup>+</sup> 672.2468, found 672.2441. HPLC: Purity  $\geq 98\%$ .

**{4-[2,3-Dichloro-4-(5-{1-[2-(2-guanidino-4-methyl-pentanoylamino)-acetyl]-piperidin-4-yl}-1-methyl-1*H*-pyrazol-3-yl)-phenoxy-methyl]-phenyl}-acetic Acid Trifluoroacetate (33h).** To **32** (60 mg, 0.10 mmol) in dimethylformamide (500  $\mu$ L) were added methyl (4-bromomethyl)phenylacetate (29 mg, 0.12 mmol) and potassium carbonate (28 mg, 0.20 mmol). The reaction mixture was stirred for 3 h at 65 °C and then diluted with ethyl acetate and washed with water. The aqueous layer was extracted with ethyl acetate (3  $\times$  2 mL), and the combined organic layer was dried over Na<sub>2</sub>SO<sub>4</sub> and concentrated under reduced pressure to obtain the ether.

The ether was dissolved in a solution of tetrahydrofuran and water (500  $\mu$ L, 3:1) and lithium hydroxide (23 mg, 1 mmol) was added. The reaction mixture was stirred at room temperature for 3 h and then was acidified using aqueous hydrochloric acid (3 mL, 1.0 M). The mixture was extracted with ethyl acetate (3  $\times$  4 mL). The combined organic layer was dried over Na<sub>2</sub>SO<sub>4</sub> and concentrated under reduced pressure to afford the acid.

The title compound was prepared according to General Procedure D. ES (+) MS  $m/e = 688$  ( $M + 1$ ).

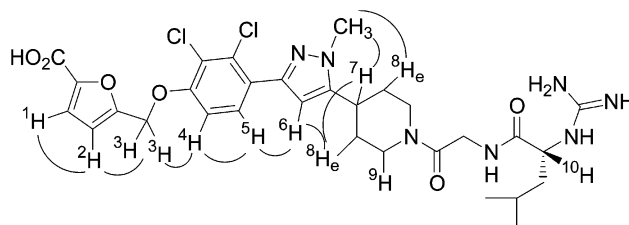
**5-Hydroxymethyl-furan-2-carboxylic Acid Methyl Ester (42).** To a solution of 5-formyl-2-furancarboxylic acid (commercially available from TCI America) (0.28 g, 2.0 mmol) in benzene/methanol (5:1, 5 mL) at room temperature was added (trimethylsilyl)diazomethane (2.0 M in hexanes, 1.0 mL, 2.0 mmol). The resulting solution was stirred at room temperature for 1 h and concentrated under reduced pressure. The residue was dissolved in methanol (2 mL) and treated with sodium borohydride (83 mg, 2.2 mmol). After 2 h, the reaction mixture was partitioned between water (20 mL) and ethyl acetate (20 mL). The aqueous layer was washed with ethyl acetate (2  $\times$  20 mL), and the combined organic layer was dried over MgSO<sub>4</sub> and concentrated under reduced pressure to afford **42** (240 mg, 77%) as a white solid. <sup>1</sup>H NMR (400 MHz, CDCl<sub>3</sub>)  $\delta$  7.13 (d, 1 H,  $J = 3.4$  Hz), 6.41 (d, 1 H,  $J = 3.4$  Hz), 4.67 (s, 2 H), 3.89 (s, 3H). ES (+) MS  $m/e = 157$  ( $M + 1$ ).

**(R)-5-[4-(5-{1-[2-(2-*tert*-Butoxycarbonylamino-4-methyl-pentanoylamino)-acetyl]-piperidin-4-yl}-1-methyl-1*H*-pyrazol-3-yl)-2,3-dichloro-phenoxy-methyl]-furan-2-carboxylic Acid (43).** To a solution of **32** (740 mg, 1.2 mmol), **42** (240 mg, 1.5 mmol), and triphenylphosphine (440 mg, 1.7 mmol) in CH<sub>2</sub>Cl<sub>2</sub> (8 mL) at room temperature was added diethyl azodicarboxylate (0.27 mL, 1.7 mmol). The resulting solution was stirred for 16 h at room temperature and was then partitioned between water and ethyl acetate. The organic layer was dried (Na<sub>2</sub>SO<sub>4</sub>) and concentrated. The crude residue was purified by flash chromatography (SiO<sub>2</sub>; 100% ethyl acetate, then 0–5% MeOH in dichloromethane) to yield 814 mg (89%) of a solid. <sup>1</sup>H NMR (400 MHz, CD<sub>3</sub>OD)  $\delta$  7.51 (d, 1 H,  $J = 8.7$  Hz), 7.23–7.21 (m, 2 H), 6.70 (d, 1 H,  $J = 3.5$  Hz),

6.44 (s, 1 H), 5.24 (s, 2 H), 4.55–4.50 (m, 1 H), 4.16–4.05 (m, 4 H), 3.89 (s, 3 H), 3.87 (s, 3 H), 3.29 (m, 1 H), 3.12 (m, 1 H), 2.88 (m, 1 H), 2.02–2.01 (m, 2 H), 1.72–1.69 (m, 2 H), 1.60–1.53 (m, 3 H), 1.44 (s, 9 H), 0.96–0.89 (m, 6 H). ES (+) MS  $m/e = 734$  ( $M + 1$ ).

To the methyl ester (814 mg, 1.10 mmol) in THF (30 mL) was added 1.0 M LiOH (1.10 mL, 1.10 mmol). The resulting mixture was stirred at room-temperature overnight and was then acidified with 1 N HCl to pH 3–4. The aqueous layer was extracted with ethyl acetate (2  $\times$  50 mL). The combined organic phases were washed with brine, dried (MgSO<sub>4</sub>), and concentrated under reduced pressure to yield 0.764 g (96%) of **43** as a colorless oil. ES (+) MS  $m/e = 720$  ( $M + 1$ ).

**(R)-5-[2,3-Dichloro-4-(5-{1-[2-(2-guanidino-4-methyl-pentanoylamino)-acetyl]-piperidin-4-yl}-1-methyl-1*H*-pyrazol-3-yl)-phenoxy-methyl]-furan-2-carboxylic Acid Trifluoroacetate (33i).** The title compound was prepared according to General Procedure D using **33**. White powder, 400 mg (41% overall for five steps from **51**). The regiochemical assignment was verified by NOE spectroscopy. (The positions of the *N*-methyl substituent and of the *O*-benzyl derivative were confirmed by NOE difference spectroscopy (400 MHz, CD<sub>3</sub>OD). Selected enhancements.) [ $\alpha$ ]<sub>D</sub> = 13.1° ( $c = 1.2$ , MeOH). <sup>1</sup>H NMR (400 MHz, DMSO-*d*<sub>6</sub>)  $\delta$  8.10 (s, 1 H), 7.85 (d, 1 H,  $J = 10.6$  Hz), 7.66 (d, 1 H,  $J = 8.8$  Hz), 7.38 (d, 1 H,  $J = 9.0$  Hz), 7.22 (d, 1 H,  $J = 3.6$  Hz), 6.81 (d, 1 H,  $J = 3.5$  Hz), 6.49 (s, 1 H), 5.32 (s, 2 H), 4.48 (d, 1 H,  $J = 10.8$  Hz), 4.25 (br s, 1 H), 4.06 (m, 2 H), 3.86 (m, 1 H), 3.81 (s, 3 H), 3.17 (app t, 1 H,  $J = 14.7$  Hz), 3.09 (app t, 1 H,  $J = 11.4$  Hz), 2.75 (app t, 1 H,  $J = 12.4$  Hz), 1.94 (d, 2 H,  $J = 10.8$  Hz), 1.58–1.41 (m, 4 H), 1.37 (m, 1 H), 0.90 (m, 6 H). <sup>1</sup>H NMR (400 MHz, CD<sub>3</sub>OD) (No NOEs between the dichlorophenol moiety and the pyrazole *N*-Me substituent were observed. Enhancements between the pyrazol/piperidine fragment and the aryloxy-methyl-furan portion were also absent.)  $\delta$  7.55 (d, 1 H,  $J = 8.7$  Hz, H-5), 7.26 (d, 1 H,  $J = 8.8$  Hz, H-4), 7.21 (d, 1 H,  $J = 3.4$  Hz, H-1), 6.71 (d, 1 H,  $J = 3.5$  Hz, H-2), 6.46 (s, 1 H, H-6), 5.26 (s, 2 H, H-3), 4.79 (d, 1 H,  $J = 13.2$  Hz, H-9ax'), 4.34–4.02 (m, 4 H, H-9ax'', COC*H*<sub>2</sub>NHCO, and H-10), 3.92 (s, 3 H, NCH<sub>3</sub>), 3.29 (m, 1 H, H-9eq'), 3.12 (m, 1 H, H-7), 2.88 (m, 1 H, H-9eq''), 2.06 (app t, 2 H,  $J = 11.2$  Hz, H-8eq), 1.75–1.60 (m, 5 H, 2 H-8ax, (Me)<sub>2</sub>CHCH<sub>2</sub>), 1.01 (m, 6 H, CH(CH<sub>3</sub>)<sub>2</sub>). Anal. (C<sub>30</sub>H<sub>37</sub>Cl<sub>2</sub>N<sub>7</sub>O<sub>6</sub>·CF<sub>3</sub>CO<sub>2</sub>H) C, H, N.



**IL-2/IL-2R $\alpha$  Inhibition Assays.** IL-2 and IL2R $\alpha$  were cloned and expressed as previously described.<sup>33</sup> Both enzyme-linked immunosorbent assay (ELISA) and scintillation proximity assay (SPA) assay were used to measure compound inhibition of IL-2/IL-2R $\alpha$ . Using two assays served as an initial check for artifacts. In general, SPA is the preferred method for monitoring weak binders because it is less artifact-prone. However, data are the same within experimental error for ELISA and SPA for compounds with IC<sub>50</sub> values <1 mM.

For ELISA, 15 nM biotinylated IL-2R $\alpha$  was immobilized in the wells of a streptavidin (Pierce Biotechnology, Rockford, IL)-coated Maxisorp 96-well plate (Corning Life Sciences). Three-fold serial dilutions of compounds were prepared in DMSO, added to a solution of 5 nM IL-2 (2% DMSO final) in Superblock (Pierce Biotechnology, Rockford, IL) with 0.01% TWEEN 20, and incubated with the immobilized IL-2R $\alpha$ . After unbound IL-2 was removed by washing, bound IL-2 was measured with 0.65 nM of an anti-IL-2 antibody labeled with horseradish peroxidase (HRP, Pierce Biotechnology, Rockford, IL) followed by addition of a colorimetric substrate for HRP (TMB, Pierce Biotechnology, Rockford, IL). The inhibition of

bound IL-2 was plotted as a function of compound concentration, and the inhibition constant ( $IC_{50}$ ) was determined by nonlinear regression analysis (Kaleidagraph, Synergy Software, Reading, PA).

For SPA, 3-fold serial dilutions of compounds were prepared in DMSO and added to 10 nM IL-2 labeled with tritiated propionic acid in 100  $\mu$ L of Superblock. This solution was then added to biotinylated IL-2R $\alpha$  bound to streptavidin-labeled scintillant-containing beads (0.7 mg/mL beads; Amersham Biosciences, Piscataway, NJ). Scintillation due to IL-2 bound to IL-2R $\alpha$  was read on a Trilux scintillation counter (Applied Biosystems, Foster City, CA).  $IC_{50}$  values were determined from curves of scintillation counts versus compound concentration using a nonlinear regression analysis.

**Surface Plasmon Resonance (SPR).** Wild-type IL-2 was immobilized on a CM5 chip (Biacore, Uppsala, Sweden) using standard amine coupling. Between 4000 and 8000 RU (refractive units) of IL-2 were immobilized; as a control, protein tyrosine phosphatase (PTP-1B) was immobilized on a separate channel. Two-fold serial dilutions of compounds were prepared in DMSO and diluted in phosphate-buffered saline (PBS) with 0.05% azide, 1% DMSO. These were injected over the IL-2/PTP-1B labeled chip at a rate of 40  $\mu$ L/min at 25 °C for 1 min. The stoichiometry of binding was estimated by eq 1 where MW is the molecular weight. The dissociation constant ( $K_{d,SPR}$ ) for each compound was determined by plotting the RU at the plateau of the binding curve versus the compound concentration; data were fit by nonlinear regression (Kaleidagraph).

$$\text{stoichiometry} = \text{RU}_{\text{ligand}} / \text{MW}_{\text{ligand}} * \text{MW}_{\text{protein}} / \text{RU}_{\text{protein}} \quad (1)$$

**Sedimentation Equilibrium Analytical Ultracentrifugation (AU).** AU measurements employed the Beckman XLA, outfitted with six-sector cells and an eight-cell rotor (Beckman Coulter, Palo Alto, CA). The experiment and fitting algorithm have been described in detail.<sup>34</sup> Briefly, compound and/or protein solutions were prepared by diluting DMSO stocks in phosphate-buffered saline to a final DMSO concentration of 1% v/v. Appropriate concentrations were chosen based on extinction coefficients and expected affinities. Samples were then measured at the following three speeds: 3K RPM scans provided extinction coefficients (via Beer's law), 25 K RPM equilibrium scans (taken after 20–24 h) provided sedimentation curves for data-fitting, and 50 K RPM equilibrium scans provided an experimental measurement of the baseline ("background" absorbance at the meniscus in protein-only samples). For each  $K_d$  determination, three ratios of compound/protein were measured simultaneously, and the three data sets were fit globally using the "Hettfitter" analysis package<sup>34</sup> and a commercially available plotting program (Igor Pro, Wavemetrics, Lake Oswego, OR).

**$^1\text{H}$ – $^{15}\text{N}$  heteronuclear Single-Quantum Coherence (HSQC) NMR.** Uniformly  $^{15}\text{N}$ -labeled IL-2 was prepared in minimal media containing  $^{15}\text{NH}_4\text{Cl}$  and exchanged into 10 mM NaOAc pH 4.5 (NAP5, Pierce Biotechnology, Rockford, IL). Samples were prepared to contain 150–200  $\mu$ M protein, 500–2000  $\mu$ M compound, and 2% DMSO.  $^1\text{H}$ – $^{15}\text{N}$  HSQC spectra were recorded on a 400-MHz Bruker Avance spectrometer (Bruker Biospin, Billerica, MA) at 39 °C. Significant shifts in the NMR spectra were observed for residues throughout the IL-2R $\alpha$  binding site and in the extended loops. Diagnostic resonances for binding at the IL-2R $\alpha$  site include those due to Glu 62 (which makes hydrogen bonds with the compounds) and Phe 42 (which undergoes large conformational changes upon binding).<sup>31,33</sup>

**Tethering.** Identifying fragments that covalently modify the Leu72Cys mutant of IL-2 has been described elsewhere.<sup>33,36</sup> Briefly, 10  $\mu$ M L72C-IL-2 in 100 mM HEPES buffer, pH 7.4, was combined with 4 mM  $\beta$ ME and 2 mM total disulfide-containing compounds (200  $\mu$ M each of 10 compounds) at a final DMSO concentration of 2%. Mixtures were allowed to come to equilibrium (2–8 h) at room temperature and then were analyzed by liquid chromatography/mass spectrometry (LC/MS). Hits were identified by the corresponding increase

in mass of the protein conjugate. Active fragments were confirmed by Tethering with 4 mM  $\beta$ ME and 200  $\mu$ M of the individual compound.

**Cell-Based Assay.** Compound activity was determined by inhibition of STAT5 phosphorylation. Cells from the mouse T-cell line CTLL-2 (gift from DNAX, Palo Alto, CA) were stimulated with human IL-2, which binds to mouse IL-2R and causes phosphorylation of the transcription factor STAT5. Cells were grown to approximately  $1 \times 10^6$  cells/mL in RPMI/IL-2 then grown without IL-2 overnight. Two-fold serial dilutions of compounds were prepared in DMSO and added to the cells in media supplemented with 0.1 ng/mL IL-2. The cell/compound mixture was incubated for 30 min at 37 °C. The amount of STAT5 phosphorylation was then measured by western blot, using phospho-STAT5 mAb (Upstate Biotechnology, Lake Placid, NY) as a primary antibody and HRP-conjugated Rabbit anti-Mouse antibody (Zymed, South San Francisco, CA) as a secondary antibody. Proliferating cell nuclear antigen (PCNA) (BD Biosciences Pharmingen, San Diego, CA) was used as a control for cell number, blot transfer, and the like. "Fractional inhibition" of STAT-5 phosphorylation was measured by densitometry of the phospho-STAT5 band and normalized by the intensity of the PCNA band. Selectivity studies monitored STAT5 phosphorylation in response to IL-15, using the analogous assay.

**Metabolic Stability and Pharmacokinetics.** The metabolic stability of **33i** was characterized by MDS Pharma Services (Bothell, WA). Pooled human liver microsomes ( $n = 15$ , 0.5 mg/mL; XenoTech, Lenexa, KS), an NADPH regenerating system, and 1  $\mu$ M compound were incubated at 37 °C. The percent of compound remaining was determined by LC/MS/MS. For pharmacokinetic measurements of **33i**, injections were performed at Northview Pacific Laboratories, Inc. (Hercules, CA), and analysis was performed in-house. Compound was formulated at 2.5 mg/mL compound in PEG 400. Groups of three male CD-1 mice per time point were treated via intravenous bolus injection (lateral tail vein) at a dose of 10 mg/kg. At serial time points, from 0.5 to 8 h, animals were sacrificed and blood was collected by cardiac puncture into sodium-EDTA tubes. Plasma was prepared by centrifugation and stored at –20 °C until analysis. Samples were analyzed using a nonvalidated LC-MS/MS method, using a plasma standard curve with appropriate quality controls for quantitation. Back-calculated standards did not deviate by more than  $\pm 15\%$  from nominal value. The average concentration (standard deviation) in  $\mu$ g/mL were as follows: 0.5 h, 7.1(3.1); 1 h, 3.6(1.6); 1.5 h, 1.4(0.5); 2 h, 1.1(0.3); 3 h, 0.46(0.17); 4 h, 0.43(0.13); 6 h, 0.16(0.06); 8 h, 0.1(0.1). Pharmacokinetic analysis was based on mean plasma concentration–time profiles. Noncompartmental analysis was performed using WinNonlin 4.0 (Pharsight Corp., Mountain View, CA).

**Acknowledgment.** The authors would like to thank J. Silverman, U. Hoch, T. Lac, and S. Prabhu for pharmacokinetic analysis, L. Taylor for protein purification, T. O'Brien for development of the STAT5 phosphorylation assay, M. Cancilla and S. Evarts for high-resolution MS analysis, and S. Lam, T. Webb, and A. Hsi for compound purification. We also thank E. M. Gordon and J. A. Wells for insightful advice.

**Supporting Information Available:** Elemental analyses data. This material is available free of charge via the Internet at <http://pubs.acs.org>.

## References

- Rubin, L. A.; Nelson, D. L. The Soluble Interleukin-2 Receptor: Biology, Function, and Clinical Application. *Ann. Intern. Med.* **1990**, *113*, 619–627.
- Nelson, B. H.; Willerford, D. M. Biology of the Interleukin-2 Receptor. *Adv. Immunol.* **1998**, *70*, 1–81.
- Waldmann, T. A.; Dubois, S.; Tagaya, Y. Contrasting Roles of IL-2 and IL-15 in the Life and Death of Lymphocytes: Implications for Immunotherapy. *Immunology* **2001**, *14*, 105–110.

- (4) Nelson, B. H. Interleukin-2 Signaling and the Maintenance of Self-Tolerance. *Curr. Dir. Autoimmun.* **2002**, *5*, 92–112.
- (5) Church, A. C. Clinical Advances in Therapies Targeting the Interleukin-2 Receptor. *Q. J. Med.* **2003**, *96*, 91–102.
- (6) Le Moine, A.; Goldman, M.; Abramowicz, D. Multiple Pathways to Allograft Rejection. *Transplantation* **2002**, *73*, 1373–1381.
- (7) Singh, V. K.; Mehrotra, S.; Agarwal, S. S. The Paradigm of Th1 and Th2 Cytokines: Its Relevance to Autoimmunity and Allergy. *Immunol. Res.* **1999**, *20*, 147–161.
- (8) Schreiber, S. L.; Crabtree, G. R. The Mechanism of Action of Cyclosporin a and Fk506. *Immunol. Today* **1992**, *13*, 136–142.
- (9) Masri, M. A. The Mosaic of Immunosuppressive Drugs. *Mol. Immunol.* **2003**, *39*, 1073–1077.
- (10) Berard, J. L.; Velez, R. L.; Freeman, R. B.; Tsunoda, S. M. A Review of Interleukin-2 Receptor Antagonists in Solid Organ Transplantation. *Pharmacotherapy* **1999**, *19*, 1127–1137.
- (11) Waldmann, T. A.; O'Shea, J. The Use of Antibodies against the Il-2 Receptor in Transplantation. *Curr. Opin. Immunol.* **1998**, *10*, 507–512.
- (12) Toogood, P. L. Inhibition of Protein-Protein Association by Small Molecules: Approaches and Progress. *J. Med. Chem.* **2002**, *45*, 1–16.
- (13) Berg, T. Modulation of Protein-Protein Interactions with Small Organic Molecules. *Angew. Chem., Int. Ed.* **2003**, *42*, 2462–2481.
- (14) Cochran, A. G. Antagonists of Protein-Protein Interactions. *Chem. Biol.* **2000**, *7*, R85–94.
- (15) Gadek, T. R.; Nicholas, J. B. Small Molecule Antagonists of Proteins. *Biochem. Pharmacol.* **2003**, *65*, 1–8.
- (16) Arkin, M. R.; Wells, J. A. Small-Molecule Inhibitors of Protein-Protein Interactions: Advancing Towards the Dream. *Nat. Rev. Drug Discovery* **2004**, in press.
- (17) Nakamura, C. E.; Abeles, R. H. Mode of Interaction of Beta-Hydroxy-Beta-Methylglutaryl Coenzyme A Reductase with Strong Binding Inhibitors: Compactin and Related Compounds. *Biochemistry* **1985**, *24*, 1364–1376.
- (18) Hajduk, P. J.; Meadows, R. P.; Fesik, S. W. Nmr-Based Screening in Drug Discovery. *Q. Rev. Biophys.* **1999**, *32*, 211–240.
- (19) Fejzo, J.; Lepre, C. A.; Peng, J. W.; Bemis, G. W.; Ajay et al. The Shapes Strategy: An Nmr-Based Approach for Lead Generation in Drug Discovery. *Chem. Biol.* **1999**, *6*, 755–769.
- (20) Boehm, H. J.; Boehringer, M.; Bur, D.; Gmuender, H.; Huber, W.; et al. Novel Inhibitors of DNA Gyrase: 3d Structure Based Biased Needle Screening, Hit Validation by Biophysical Methods, and 3d Guided Optimization. A Promising Alternative to Random Screening. *J. Med. Chem.* **2000**, *43*, 2664–2674.
- (21) Liu, G.; Huth, J. R.; Olejniczak, E. T.; Mendoza, R.; DeVries, P. et al. Novel P-Arylthio Cinnamides as Antagonists of Leukocyte Function-Associated Antigen-1/Intracellular Adhesion Molecule-1 Interaction. 2. Mechanism of Inhibition and Structure-Based Improvement of Pharmaceutical Properties. *J. Med. Chem.* **2001**, *44*, 1202–1210.
- (22) Carr, R.; Jhoti, H. Structure-Based Screening of Low-Affinity Compounds. *Drug Discovery Today* **2002**, *7*, 522–527.
- (23) Erlanson, D. A.; Wells, J. A.; Braisted, A. C. Tethering: Fragment-Based Drug Discovery. *Annu. Rev. Biophys. Biomol. Struct.* **2004**, *33*, in press.
- (24) Hann, M. M.; Leach, A. R.; Harper, G. Molecular Complexity and Its Impact on the Probability of Finding Leads for Drug Discovery. *J. Chem. Inf. Comput. Sci.* **2001**, *41*, 856–864.
- (25) Jahnke, W.; Florshheimer, A.; Blommers, M. J.; Paris, C. G.; Heim, J.; et al. Second-Site NMR Screening and Linker Design. *Curr. Top. Med. Chem.* **2003**, *3*, 69–80.
- (26) Nienaber, V. L.; Richardson, P. L.; Klighofer, V.; Bouska, J. J.; Giranda, V. L.; et al. Discovering Novel Ligands for Macromolecules Using X-ray Crystallographic Screening. *Nat. Biotechnol.* **2000**, *18*, 1105–1108.
- (27) Maly, D. J.; Choong, I. C.; Ellman, J. A. Combinatorial Target-Guided Ligand Assembly: Identification of Potent Subtype-Selective C-Src Inhibitors. *Proc. Natl. Acad. Sci. U.S.A.* **2000**, *97*, 2419–2424.
- (28) Vetter, D. Chemical Microarrays, Fragment Diversity, Label-Free Imaging by Plasmon Resonance—a Chemical Genomics Approach. *J. Cell Biochem. Suppl.* **2002**, *39*, 79–84.
- (29) Hyde, J.; Braisted, A. C.; Randal, M.; Arkin, M. R. Discovery and Characterization of Cooperative Ligand Binding in the Adaptive Region of Interleukin-2. *Biochemistry* **2003**, *42*, 6475–6483.
- (30) Erlanson, D. A.; Braisted, A. C.; Raphael, D. R.; Randal, M.; Stroud, R. M.; et al. Site-Directed Ligand Discovery. *Proc. Natl. Acad. Sci. U.S.A.* **2000**, *97*, 9367–9372.
- (31) Tilley, J. W.; Chen, L.; Fry, D. C.; Emerson, S. D.; Powers, G. D.; et al. Identification of a Small Molecule Inhibitor of the Il-2/Il-2alpha Receptor Interaction Which Binds to Il-2. *J. Am. Chem. Soc.* **1997**, *119*, 7589–7590.
- (32) Emerson, S. D.; Palermo, R.; Liu, C. M.; Tilley, J. W.; Chen, L.; et al. NMR Characterization of Interleukin-2 in Complexes with the Il-2alpha Receptor Component, and with Low Molecular Weight Compounds That Inhibit the Il-2/Il-2alpha Interaction. *Protein Sci.* **2003**, *12*, 811–822.
- (33) Arkin, M. R.; Mike, R.; Delano, W. L.; Hyde, J.; Luong, T. N. et al. Binding of Small Molecules to an Adaptive Protein: Protein Interface. *Proc. Natl. Acad. Sci. U.S.A.* **2003**, *100*, 1603–1608.
- (34) Arkin, M.; Lear, J. D. A New Data Analysis Method to Determine Binding Constants of Small Molecules to Proteins Using Equilibrium Analytical Ultracentrifugation with Absorption Optics. *Anal. Biochem.* **2001**, *299*, 98–107.
- (35) Thanos, C.; Randal, M.; Wells, J. A. Potent Small-Molecule Binding to a Dynamic Hot Spot on Il-2. *J. Am. Chem. Soc.* **2003**, *125*, 15280–15281.
- (36) Braisted, A. C.; Oslob, J. D.; Delano, W. L.; Hyde, J.; McDowell, R. S.; et al. Discovery of a Potent Small Molecule Il-2 Inhibitor through Fragment Assembly. *J. Am. Chem. Soc.* **2003**, *125*, 3714–3715.
- (37) Johnston, J. A.; Bacon, C. M.; Finbloom, D. S.; Rees, R. C.; Kaplan, D.; et al. Tyrosine Phosphorylation and Activation of Stat5, Stat3, and Janus Kinases by Interleukins 2 and 15. *Proc. Natl. Acad. Sci. U.S.A.* **1995**, *92*, 8705–8709.
- (38) McKay, D. B. Unraveling the Structure of Interleukin-2: Reply. *Science* **1992**, *257*, 412–413.
- (39) Mott, H. R.; Baines, B. S.; Hall, R. M.; Cooke, R. M.; Driscoll, P. C.; et al. The Solution Structure of the F42a Mutant of Human Interleukin 2. *J. Mol. Biol.* **1995**, *247*, 979–994.
- (40) Hajduk, P. J.; Gomtsyan, A.; Didomenico, S.; Cowart, M.; Bayburt, E. K.; et al. Design of Adenosine Kinase Inhibitors from the Nmr-Based Screening of Fragments. *J. Med. Chem.* **2000**, *43*, 4781–4786.
- (41) Bogan, A. A.; Thorn, K. S. Anatomy of Hot Spots in Protein Interfaces. *J. Mol. Biol.* **1998**, *280*, 1–9.
- (42) Lo Conte, L.; Chothia, C.; Janin, J. The Atomic Structure of Protein-Protein Recognition Sites. *J. Mol. Biol.* **1999**, *285*, 2177–2198.
- (43) Wells, J. A.; de Vos, A. M. Hematopoietic Receptor Complexes. *Annu. Rev. Biochem.* **1996**, *65*, 609–634.
- (44) Atwell, S.; Ultsch, M.; De Vos, A. M.; Wells, J. A. Structural Plasticity in a Remodeled Protein-Protein Interface. *Science* **1997**, *278*, 1125–1128.
- (45) DeLano, W. L.; Ultsch, M. H.; de Vos, A. M.; Wells, J. A. Convergent Solutions to Binding at a Protein-Protein Interface. *Science* **2000**, *287*, 1279–1283.
- (46) Ma, B.; Shatsky, M.; Wolfson, H. J.; Nussinov, R. Multiple Diverse Ligands Binding at a Single Protein Site: A Matter of Preexisting Populations. *Protein. Sci.* **2002**, *11*, 184–197.
- (47) Sundberg, E. J.; Mariuzza, R. A. Luxury Accommodations: The Expanding Role of Structural Plasticity in Protein-Protein Interactions. *Structure Fold. Des.* **2000**, *8*, R137–142.
- (48) Freire, E. The Propagation of Binding Interactions to Remote Sites in Proteins: Analysis of the Binding of the Monoclonal Antibody D1.3 to Lysozyme. *Proc. Natl. Acad. Sci. U.S.A.* **1999**, *96*, 10118–10122.
- (49) McGovern, S. L.; Helfand, B. T.; Feng, B.; Shoichet, B. K. A Specific Mechanism of Nonspecific Inhibition. *J. Med. Chem.* **2003**, *46*, 4265–4272.
- (50) McGovern, S. L.; Caselli, E.; Grigorieff, N.; Shoichet, B. K. A Common Mechanism Underlying Promiscuous Inhibitors from Virtual and High-Throughput Screening. *J. Med. Chem.* **2002**, *45*, 1712–1722.
- (51) Iyobe, A.; Uchida, M.; Kamata, K.; Hotei, Y.; Kusama, H. et al. Studies on New Platelet Aggregation Inhibitors 1. Synthesis of 7-Nitro-3,4-Dihydroquinoline-2(1H)-one Derivatives. *Chem. Pharm. Bull. (Tokyo)* **2001**, *49*, 822–829.
- (52) Klein, S. I.; Molino, B. F.; Czekaj, M.; Gardner, C. J.; Chu, V.; et al. Design of a New Class of Orally Active Fibrinogen Receptor Antagonists. *J. Med. Chem.* **1998**, *41*, 2492–2502.
- (53) Muller, S.; Liepold, B.; Roth, G. J.; Bestmann, H. J. An Improved One-Pot Procedure for the Synthesis of Alkynes from Aldehydes. *Synlett* **1996**, 521–522.
- (54) Sauve, K.; Nachman, M.; Spence, C.; Bailon, P.; Campbell, E.; et al. Localization in Human Interleukin 2 of the Binding Site to the Alpha Chain (P55) of the Interleukin 2 Receptor. *Proc. Natl. Acad. Sci. U.S.A.* **1991**, *88*, 4636–4640.
- (55) Zurawski, S. M.; Vega, F., Jr.; Doyle, E. L.; Huyghe, B.; Flaherty, K.; et al. Definition and Spatial Location of Mouse Interleukin-2 Residues That Interact with Its Heterotrimeric Receptor. *Embo J.* **1993**, *12*, 5113–5119.